Journal of Archaeological Science: Reports 53 (2024) 104406

Contents lists available at ScienceDirect

Journal of Archaeological Science: Reports

journal homepage: www.elsevier.com/locate/jasrep

Local and exotic sources of sarsen debitage at Stonehenge revealed by geochemical provenancing

T. Jake R. Ciborowski [a,*], David J. Nash [b,c], Timothy Darvill [d], Ben Chan [d], Mike Parker Pearson [e], Rebecca Pullen [f], Colin Richards [g], Hugo Anderson-Whymark [h]

[a] Earth and Life Sciences, School of Natural Sciences, University of Galway, Galway, Republic of Ireland
[b] School of Applied Sciences, University of Brighton, Brighton, United Kingdom
[c] School of Geography, Archaeology and Environmental Studies, University of the Witwatersrand, Johannesburg, South Africa
[d] Department of Archaeology and Anthropology, Bournemouth University, Poole, Dorset, United Kingdom
[e] Institute of Archaeology, University College London, London, United Kingdom
[f] Archaeological Investigation Team, Historic England, York, United Kingdom
[g] Archaeology Institute, Orkney College, University of the Highlands and Islands, Kirkwall, United Kingdom
[h] Scottish History and Archaeology, National Museums Scotland, Chambers Street, Edinburgh, United Kingdom

ARTICLE INFO

Keywords:
Stonehenge
Sarsen
Silcrete
Geochemical provenancing
pXRF
ICP-AES
ICP-MS

ABSTRACT

The application of novel geochemical provenancing techniques has changed our understanding of the construction of Stonehenge, by identifying West Woods on the Marlborough Downs as the likely source area for the majority of the extant sarsen megaliths at the monument. In this study, we apply the same techniques to saccharoid sarsen fragments from three excavations within and outwith the main Sarsen Circle to expand our understanding of the provenance of sarsen debitage present at the monument. Through pXRF analysis, we demonstrate that the surface geochemistry of 1,028 excavated sarsen fragments is significantly affected by subsurface weathering following burial in a way that cannot be overcome by simple cleaning. However, we show that this effect is surficial and does not have a volumetrically significant impact, thus permitting the subsequent use of whole-rock analytical methods. Comparison of ICP-AES and ICP-MS trace element data from 54 representative sarsen fragments with equivalent data from Stone 58 at Stonehenge demonstrates that none are debitage produced during the dressing of this megalith or its 49 chemical equivalents at the monument. Further inspection of the ICP-MS data reveals that 22 of these fragments fall into three distinct geochemical 'families'. None of these families overlap with the geochemical signature of Stone 58 and its chemical equivalents, implying that sarsen imported from at least a further three locations (in addition to West Woods) is present at Stonehenge.

Comparison of immobile trace element signatures from the 54 excavated sarsen fragments against equivalent data for 20 sarsen outcrop areas across southern Britain shows that 15 of the fragments can be linked to specific localities. Eleven of these were likely sourced from Monkton Down, Totterdown Wood and West Woods on the Marlborough Downs (25–33 km north of Stonehenge). Three fragments likely came from Bramdean, Hampshire (51 km southeast of Stonehenge), and one from Stoney Wish, East Sussex (123 km to the southeast). Technological analysis and refitting shows that one of the fragments sourced from Monkton Down was part of a 25.7 cm × 17.9 cm flake removed from the outer surface of a large sarsen boulder, most probably during on-site dressing. This adds a second likely source area for the sarsen megaliths at Stonehenge in addition to West Woods. At this stage, we can only speculate on why sarsen from such diverse sources is present at Stonehenge. We do not know whether the fragments analysed by ICP-MS were removed from (i) the outer surface of Stones 26 or 160 (which are chemically distinct to the other extant sarsen megaliths), (ii) one of the c.28 sarsen megaliths and lintels from the c.60 erected during Stage 2 of the construction of Stonehenge that may now be missing from the monument, or (iii) one of the dismantled and destroyed sarsen megaliths associated with Stage 1 of the monument. With the exception of the fragment sourced from Monkton Down, it is also possible that the analysed fragments were (iv) pieces of saccharoid sarsen hammerstones or their pre-forms, or (v) small blocks brought on-site for ceremonial or non-ceremonial purposes.

* Corresponding author.
E-mail address: jake.ciborowski@universityofgalway.ie (T.J.R. Ciborowski).

https://doi.org/10.1016/j.jasrep.2024.104406
Received 18 August 2023; Received in revised form 11 January 2024; Accepted 18 January 2024
Available online 26 January 2024
2352-409X/© 2024 The Author(s). Published by Elsevier Ltd. This is an open access article under the CC BY license (http://creativecommons.org/licenses/by/4.0/).

1. Introduction

Situated on the Chalk downlands of Salisbury Plain in southern Britain, Stonehenge is arguably the most iconic Neolithic monument in the world. The first identified stage in the structures still visible on the site today began around 3000 cal BCE with the construction of a circular earthwork enclosure bounded by a ditch and internal bank (see Fig. 1), and the digging of a circle of 56 'Aubrey Holes' (pits) around the inner edge of the bank. The main sarsen structures – the Trilithon Horseshoe, Sarsen Circle and the Station Stone Rectangle – belong to Stage 2 of the monument's construction and were set up during the period 2620–2480 cal BCE (Darvill et al., 2012; Parker Pearson et al., 2020).

One of the debates about Stonehenge centres around the source provenance of the stones. The majority of the non-sarsen stones (known as the Bluestones) have long been linked to a series of source outcrops in the Preseli Hills of west Wales using data from archaeological, petrological, and geochemical studies (e.g. Thorpe et al., 1991; Bevins et al., 2011; Bevins et al., 2012; Bevins et al., 2014; Darvill and Wainwright, 2014; Parker Pearson et al., 2015; Bevins et al., 2020; Bevins et al., 2022; Pearce et al., 2022). Until recently, however, there had been little research into the provenance of the 52 extant sarsens at the monument (see Howard, 1982, for an exception). This changed in 2020, when Nash et al. (2020) used portable X-ray fluorescence spectrometry (pXRF) data to show that all except two of the extant sarsens share a common chemical composition, and hence a common source. Inductively-coupled plasma mass spectrometry (ICP-MS) data from Stone 58 (see Fig. 1) – itself representative of the main compositional group – was compared with equivalent geochemical data from 20 areas of natural sarsen 'outcrop' across southern Britain to demonstrate that the main source of the extant Stonehenge sarsens was most likely West Woods, 25

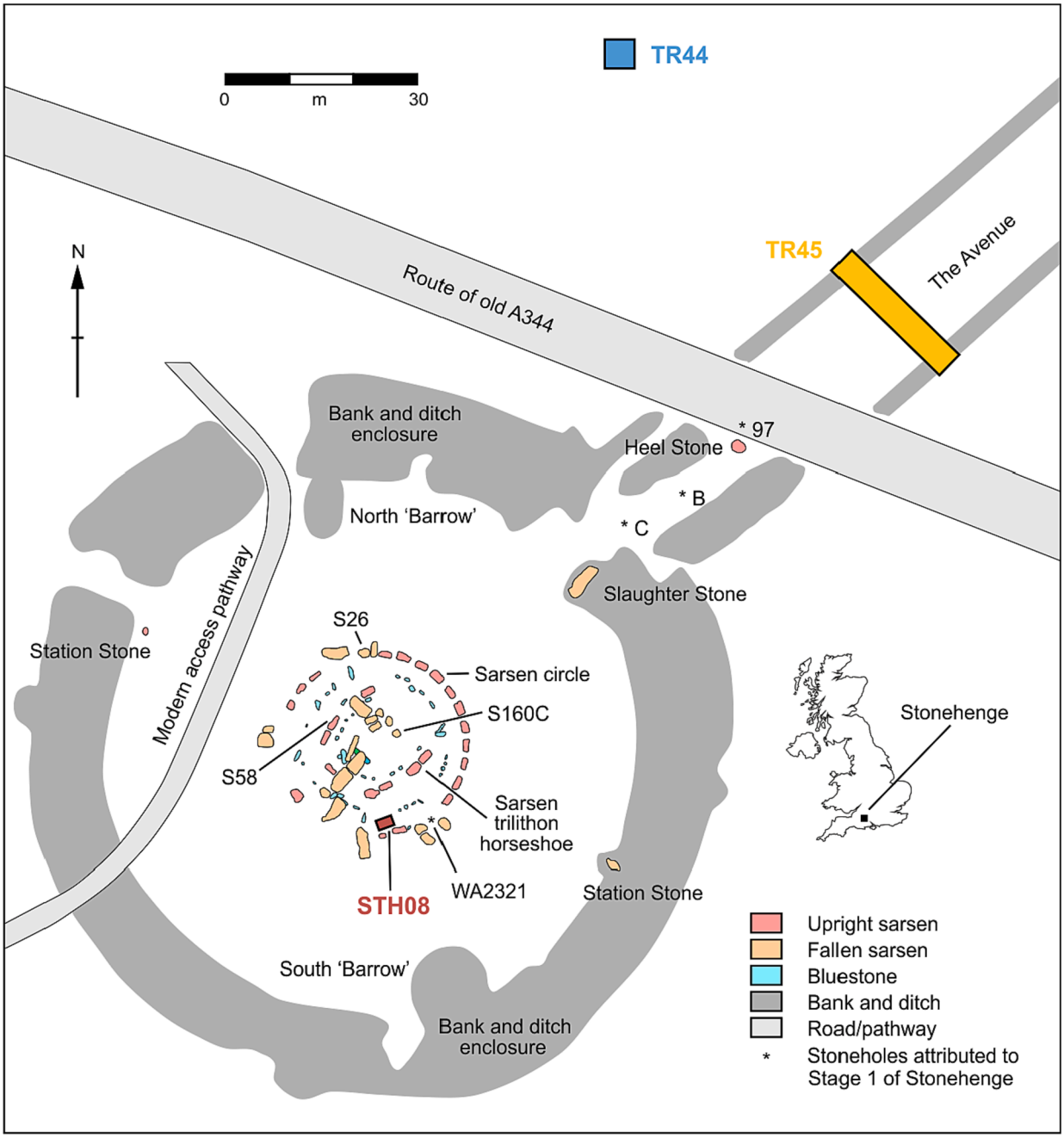

Fig. 1. Plan of Stonehenge, showing locations of STH08 and SAV08 (trenches TR44 and TR45) from which the sarsen debitage analysed in this study was excavated.

km north of the monument in the Marlborough Downs.

The source provenance of the two compositionally distinct sarsens at Stonehenge (upright Stone 26 and lintel Stone 160) is unknown and will likely remain unknown until it is possible to analyse samples from the interior of these stones. There is, however, considerable potential to use geochemical analysis of debitage unearthed during excavations at the monument to explore the source provenance of other sarsen material brought to the site. As discussed in Section 2, this debitage may derive from various sources: it may be material removed from the outer surface of extant or missing sarsen megaliths, prior to and/or during their erection in Stage 2 of the monument's construction (see Abbott and Anderson-Whymark, 2012), or the remains of broken hammerstones, or fragments of smaller blocks brought to the site. Alternatively, it could be broken fragments of missing sarsen megaliths dating to before Stage 2. Ixer and Bevins (2021) have recently demonstrated the petrographic variability of sarsen debitage in the wider Stonehenge landscape – here we use geochemical data to identify whether sarsens from source areas other than West Woods may be present at the monument.

The study applies a combination of geochemical and statistical approaches to sarsen debitage from three excavations within and outwith the main Sarsen Circle at Stonehenge (see Section 2). These approaches have been used elsewhere (e.g. Nash et al., 2013; Nash et al., 2016; Nash et al., 2022) to provide definitive geochemical matches between lithic artefacts and source outcrops, and in so doing, empirically constrain artefact-source provenance.

We first use pXRF spectrometry to provide a geochemical characterisation of 1,028 sarsen fragments sampled from across the three excavations. This includes an in-depth analysis of a larger sarsen block with an outer subsoil-weathered patina, to assess the extent to which weathering following burial may have altered the composition of the stone and hence affected its chemistry. (Note that we use the term *subsoil-weathered patina* here to describe a patina developed on a sarsen fragment as a result of weathering in the subsoil environment, as distinct from one developed on the surface of a natural sarsen boulder or dressed sarsen megalith exposed to *subaerial* weathering.) We then present ICP-MS and ICP-atomic emission spectrometry (ICP-AES) data for a subset of fragments selected from across the geochemical space defined by the pXRF data. The ICP-MS and ICP-AES data are first analysed to identify chemically distinct sarsen groupings within the subset of fragments. These data are then compared to equivalent data from Stone 58 at Stonehenge and sarsen outcrops across southern Britain to answer two questions: (i) does the analysed sarsen debitage derive from the on-site dressing of Stone 58 (or, by inference, any of the 49 other extant sarsen megaliths at Stonehenge with a similar chemical composition); and (ii) what was the original source provenance of the sarsen debitage? We then consider the outstanding questions posed by these new data and the wider methodological implications for future archaeological provenancing studies.

2. Background to the Stonehenge excavations

The sarsen fragments studied here are sourced from trenches excavated by teams led by: (i) authors MPP, CR, RP and BC, as part of the Stonehenge Riverside Project that ran between 2003 and 2009 (site-code SAV08, trenches 44 and 45 [henceforth TR44 and TR45], to the north and northeast of Stonehenge; Parker Pearson et al., 2020); and (ii) author TD, as part of the SPACES project in 2008 (site-code STH08, within the Sarsen Circle; Darvill and Wainwright, 2009). In each of these trenches (see Fig. 1 for locations), significant amounts of lithic debitage were recovered, spanning the rock types represented by the extant standing stones at the monument. The presence of debitage in these excavations has been interpreted as evidence that many of the standing stones at Stonehenge were dressed (or re-dressed) on-site prior to being erected (Pitts, 1982; Parker Pearson et al., 2017).

Historically, sarsens in southern Britain have been divided into two types, namely 'hard' sarsen (sometimes referred to as 'quartzite sarsen' in the archaeological literature) and 'saccharoid' sarsen (on the basis of its appearance resembling "that of a broken loaf-sugar"; Jones, 1887). This terminology is continued here. Fragments of both types have been excavated during investigations at Stonehenge. Saccharoid sarsen was used largely to form the uprights and lintel stones at the monument, whereas hard sarsen was primarily used for hammerstones; of 190 hammerstones from Stonehenge, only 4% are of saccharoid sarsen compared with 86% of hard sarsen (see Chan et al., 2020: 342).

2.1. The TR44 and TR45 excavations

Trenches 44 and 45 were excavated in 2008, with the excavation of TR44 directed by authors BC and CR, and TR45 by authors MPP and RP. TR44 (5 m by 5 m) was sited 70 m north of Stonehenge to examine a possible sarsen-dressing area. An assemblage of 34,941 pieces of sarsen, weighing 282 kg, was recovered from the trench; this includes 21,888 pieces of hard sarsen and 13,053 pieces of saccharoid sarsen. Sarsen debris occurred mainly in the west of the trench and tailed off abruptly across a north–south line in the eastern third of the trench (see Fig. 6.10 in Chan et al., 2020). The assemblage is interpreted as comprising (i) debris from hammerstones, and (ii) reduction waste from dressing a large sarsen block that had once lain in the eastern part of the trench and against which most of the debris had accumulated (Chan et al., 2020: 315). Alongside the mass of sarsen debitage, the artefacts in TR44 included 283 hard sarsen hammerstones, and 9 hammerstones of saccharoid sarsen (see Table 6.2 in Chan et al., 2020). The ratio of hammerstones of hard sarsen to saccharoid sarsen, together with the identification of 8 pieces of saccharoid sarsen with pecked or ground surfaces, and a small number of large (>10 cm) saccharoid sarsen flakes, suggests that the saccharoid sarsen fragments in TR44 are remnants from the prehistoric dressing of a megalithic block. It is difficult to determine how many of the saccharoid sarsen fragments derive from peck-dressing or flaking. However, given the limited number of large flakes and the fact that the hammerstones in the assemblage were of a size that could be held in one hand (Chan et al., 2020: 313), it appears that the primary activity taking place in the area of TR44 was fine flaking and peck-dressing, as opposed to the rough shaping of a boulder through the removal of large flakes.

TR45 (26 m by 4 m) was dug across the width of the Stonehenge Avenue, 60 m from the northeast entrance to Stonehenge, to investigate the Avenue's construction. Its 2 m-wide northeastern half had originally been excavated in 1956 by Richard Atkinson (Cleal et al., 1995: 309-311). An assemblage of 3,496 sarsen pieces weighing 75 kg was recovered from this trench. Of the stratified material, 38% came from the fills of two conjoining pits under the Avenue, 32% from the makeup layers of the Avenue banks, and 15% from buried soils beneath the Avenue banks (Chan et al., 2020: 321). The material from the two pits is associated with an antler pick dating to 2310–2200 cal BCE during Stage 3 of the construction of Stonehenge, whereas the material from within or under the banks can be dated to before 2580–2280 cal BCE (see Table 8.1 and discussion in Marshall et al., 2020). The lower and uneven density of debris in TR45 suggests that sarsen-dressing took place not here but nearby, perhaps to the southeast. The hammerstones in TR45 are similar in size to those in TR44 (Chan et al., 2020: 328), so this dressing is again likely to have been dominated by peck-dressing and fine flaking.

In both trenches the material was recovered by dry-sieving through a 10 mm mesh, with the sarsen layer (Context 006) in TR44 and the conjoining pit fills in TR45 being sieved through a 5 mm mesh. Finds were recorded on a 0.5 m and a 1.0 m grid in TR44 and TR45 respectively and given a context number, a square number and, for significant items, a find number.

2.2. The STH08 excavation

The STH08 excavation, directed by author TD and the late Geoff Wainwright, comprised a 2.5 m by 3.5 m trench sited between the Sarsen

Circle and the Trilithon Horseshoe in the southeast sector of the circle (Fig. 1). Its purpose was to investigate the remains of the Outer Bluestone Circle and associated features connected with the construction of the sarsen elements of the monument. An interim report (Darvill and Wainwright, 2009) outlines the main sequence of deposits uncovered. An assemblage of approximately 2,700 pieces of sarsen weighing about 26.4 kg was recovered from the excavation as recorded finds. Sampled finds are referred to by their context number (C) alongside a find number (FN) and/or environmental sample (ES) number.

The northern part of the trench included the re-excavation of cuttings made by Richard Atkinson in 1964 and the backfill of this feature (context C2). The fill included discarded sarsen fragments from a range of features that he was exploring in that season, including packing stones from around Stones 53 and 54 forming the southeastern Trilithon, debitage from stone dressing, and hammerstones. The material accounted for nearly 30% by weight but only about 4% by number of the overall recorded finds assemblage. C2 was excavated in a series of spits and was also divided into a grid, hence some find codes include a spit number. A second major source of sarsen fragments was the so-called 'Stonehenge Layer' (C3), which is an old ground surface around and between the stones that slowly accumulated between prehistoric times and the mid twentieth century CE when it was sealed below make-up for the present ground surface. Sarsen from this context accounts for about 36% by weight and nearly 62% by number of fragments. Also rich in sarsen was C12, the fill of a large Roman pit that accounted for 20% by weight and nearly 15% by number. Other contexts yielded only small amounts of sarsen, but notably include the sockets of sarsen Stone 9 (C15-C20) and Stone 10 (C25-C26 and C37-C38) in the Sarsen Circle.

3. Materials and methods

In this section, we detail the approach used to sample sarsen debitage from TR44, TR45 and STH08, and the methods used to determine sarsen geochemistry. All reported work was carried out under the terms of the post-excavation agreements with the National Trust and English Heritage for the Stonehenge Riverside and SPACES projects. Saccharoid sarsen is the only type in the UK for which high-resolution ICP-MS and ICP-AES data are currently available (see Nash et al., 2021b). For this reason, fragments of hard sarsen were identified and excluded from subsequent analyses, such that – within the limits of visual petrographic inspection – only data for saccharoid sarsen fragments are presented here. The interrogation, visualisation and presentation of all geochemical data was carried out using Microsoft Excel.

3.1. pXRF analysis

Standard XRF analysis is usually conducted on fused glass beads or homogenised powders, and involves the destruction of samples. Portable XRF, however, is entirely non-destructive, in terms of both its sample preparation and its analysis, and can be used on samples 'as is'. For this reason, and others including the relatively low cost and speed of data acquisition, pXRF is widely used in archaeological studies (e.g. Frankel and Webb, 2012; Frahm, 2013; Frahm and Doonan, 2013; Frahm et al., 2016; Tykot, 2016), including in investigations of silcrete/sarsen (e.g. Cochrane et al., 2017; Nash et al., 2020; Nash et al., 2021a). In this study, we use pXRF to provide: (i) an initial geochemical characterisation of a sample set of sarsen debitage from the three trenches, to determine the extent of compositional variability within and between each assemblage, and within an individual large sarsen block; and (ii) a dataset to compare against the pXRF results from sarsen uprights and lintels at Stonehenge reported in Nash et al. (2020).

3.1.1. Sampling of sarsen debitage

Sampling of sarsen debitage for geochemical analysis was undertaken at the University of Brighton. Sarsen had already been separated out during post-excavation analysis of the STH08 assemblage, so the entire sarsen component was transported intact. Technological analyses have not been conducted on these sarsen fragments. For TR44, the majority of sarsen debris was reburied in the trench at the end of the excavation, with a sample retained for future analysis. This included fragments that were deemed to be of interest technologically (e.g. pieces with pecked surfaces or clear flake attributes), alongside a general selection of material from across the trench. The current analysis was conducted on a random selection from this retained sample. Technological cataloguing of the selected artefacts from TR44 by author BC showed that 62.5% of the pieces are flakes of >5 cm in length and one piece is a flake with a pecked outer surface. Many of the flakes, and especially the pecked flake, are likely to be dressing debris rather than fragments of broken hammerstones. This is most certainly the case for a group of five flakes with dimensions >10 cm. The clearest example of these is a broken flake from TR44, Context 006, Square 74/1 (Fig. 2). During excavation, the conjoining pieces of this flake were found in different parts of the same 0.5 m square, suggesting that the flake was left on the ground close to the point at which it was struck from a sarsen boulder. The refitted flake measures 25.7 cm $\times$ 17.9 cm. The flake lacks an outer weathered cortex on its dorsal surface, which carries a clear flake scar; taken together, this indicates that the flake was part of a sequence of flake removals. The technological character of the flake indicates that it was removed as part of the intentional dressing of a large sarsen block. For TR45, all the sarsen debris was retained for future analysis; a random selection for chemical analysis was made of fragments likely to be dressing debris.

At Brighton, each sarsen fragment was cleaned using tap water, standard kitchen detergent and a nylon brush to remove any adhered plant and soil material from the stone surface, and then air-dried. Despite these efforts, samples retained a variably orange-brown subsoil-weathered patina. More stringent chemical cleaning solutions were not used. This was to avoid the differential alteration of the primary mineralogy of the stone, which could potentially affect the pXRF results (and those of whole-rock analyses – see Section 3.2) more than the presence of the patina.

The cleaned sarsen fragments were screened by size, with each fragment ≥ 30 mm across (i.e. sufficiently large to cover the detector window of the pXRF instrument) selected for geochemical analysis. This resulted in a sample of 1,028 fragments from the three assemblages (TR44 – 71 fragments; TR45 – 367 fragments; STH08 – 590 fragments). For ease of reference in the laboratory, the fragments were renumbered into a single sequence. **Table S1** in the Supplementary Online Information (SOM) details the conversion from our laboratory numbers to original archaeological recording numbers.

In addition to the 1,028 selected sarsen fragments, a block of sarsen excavated from trench STH08 (sample *STH08 C2 (Spit 3) FN549*, dimensions 15.7 cm $\times$ 8.3 cm $\times$ 6.9 cm) was chosen for in-depth analysis (Fig. 3). The aim of this analysis was to determine: (i) if any difference existed between the primary geochemical composition of the unweathered interior of the block and its patinated outer surface; and (ii) the depth to which any weathering effect may have penetrated into the stone surface. Sample *STH08 C2 (Spit 3) FN549* was selected for three reasons. First, it has a typical saccharoid sarsen texture. Second, it retained a visible subsoil-weathered patina, even after cleaning. Third, it is sufficiently large to have retained an unweathered interior under the soil weathering conditions experienced over the likely c.4500 years since burial.

3.1.2. pXRF methodology

Three analyses were taken at random points on the surface of each sarsen fragment using a handheld Olympus Innov-X Delta Professional XRF spectrometer at the University of Brighton. This generated 3,084 data points in total. The model operates at 40 kV, is equipped with a Rh anode 4 W X-Ray tube, and uses a silicon drift detector. The 'Geochem' mode was used for all pXRF analyses; this captures data for 34 elements (Mg, Al, Si, P, S, K, Ca, Ti, V, Cr, Mn, Fe, Co, Ni, Cu, Zn, As, Se, Rb, Sr, Y,

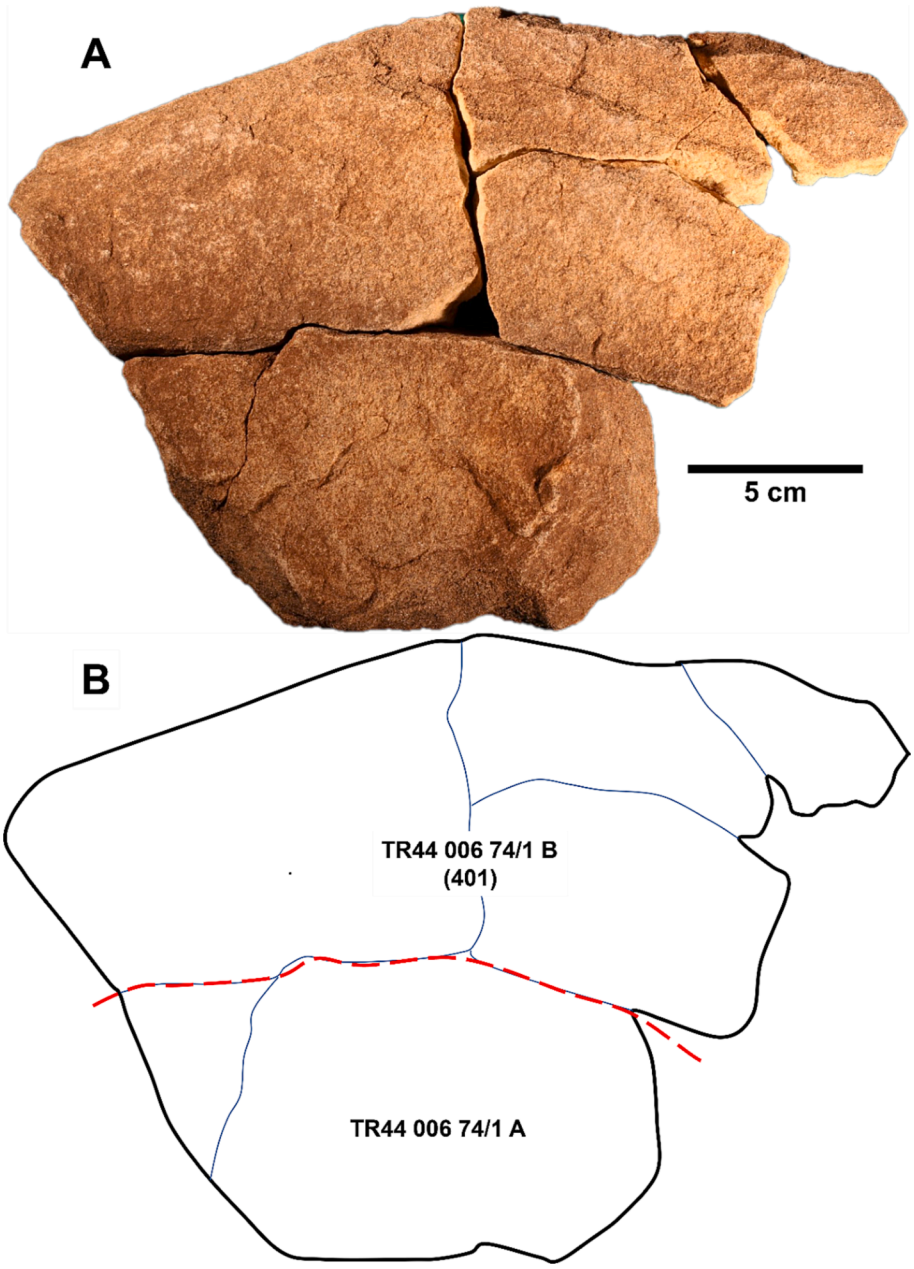

Fig. 2. A - Photograph of refitted sarsen sample *SAV08 TR44 006 74/1* from trench TR44. B – Schematic, showing principal fractures and delineation into parts A and B (dashed line). The join between the two parts was weathered, suggesting that the flake was fragmented in prehistory. All the fragments were found in the same 0.5 m square. A subsample of part B was analysed via ICP-AES and ICP-MS as sample 401.

Zr, Nb, Mo, Ag, Cd, Sn, Sb, W, Hg, Pb, Bi, U and Th). At each point on the sarsen surface, the stone was analysed for 120 s of total exposure. The device was positioned such that the detector window was completely covered by the stone, with the surface of each fragment as close to perpendicular to the beam direction as possible. After every twelve analyses (i.e. after four fragments had been analysed in triplicate), a calibration check was made against a 316 Stainless Steel Calibration Check Reference Coin to ensure accuracy and consistency of the results.

Analysis of sample *STH08 C2 (Spit 3) FN549* used the protocols described above, but with the number of exterior surface analyses increased to 25. Following surface analysis, the block was sliced using a diamond-bladed rock saw to expose its interior. The fresh cut surface was analysed seven times at random points, with a lateral straight-line transect (comprising 18 analyses at 7 mm intervals) taken across the cut surface from weathered patina to weathered patina.

3.2. ICP-MS and ICP-AES analyses

ICP spectrometry is a more costly and time-intensive method than pXRF, and the destructive nature of sample preparation is an inhibiting factor for certain archaeological analyses. However, ICP methods are far more sensitive than pXRF and allow analysis of concentrations down to parts per billion scale across a much wider range of petrologically 'useful' elements. In this study, we use ICP-AES and ICP-MS analyses to: (i) provide a full geochemical characterisation of a representative selection of sarsen fragments from TR44, TR45 and STH08; and (ii) allow direct comparison of our dataset with equivalent data from sarsen upright Stone 58 at Stonehenge and sarsen outcrops at 20 sites across southern Britain (see Nash et al., 2020). The comparator data in (ii) were generated at the same laboratory as this study, using the same instruments and protocols for sample preparation and analysis, and are available from the Archaeology Data Service (Nash et al., 2021b).

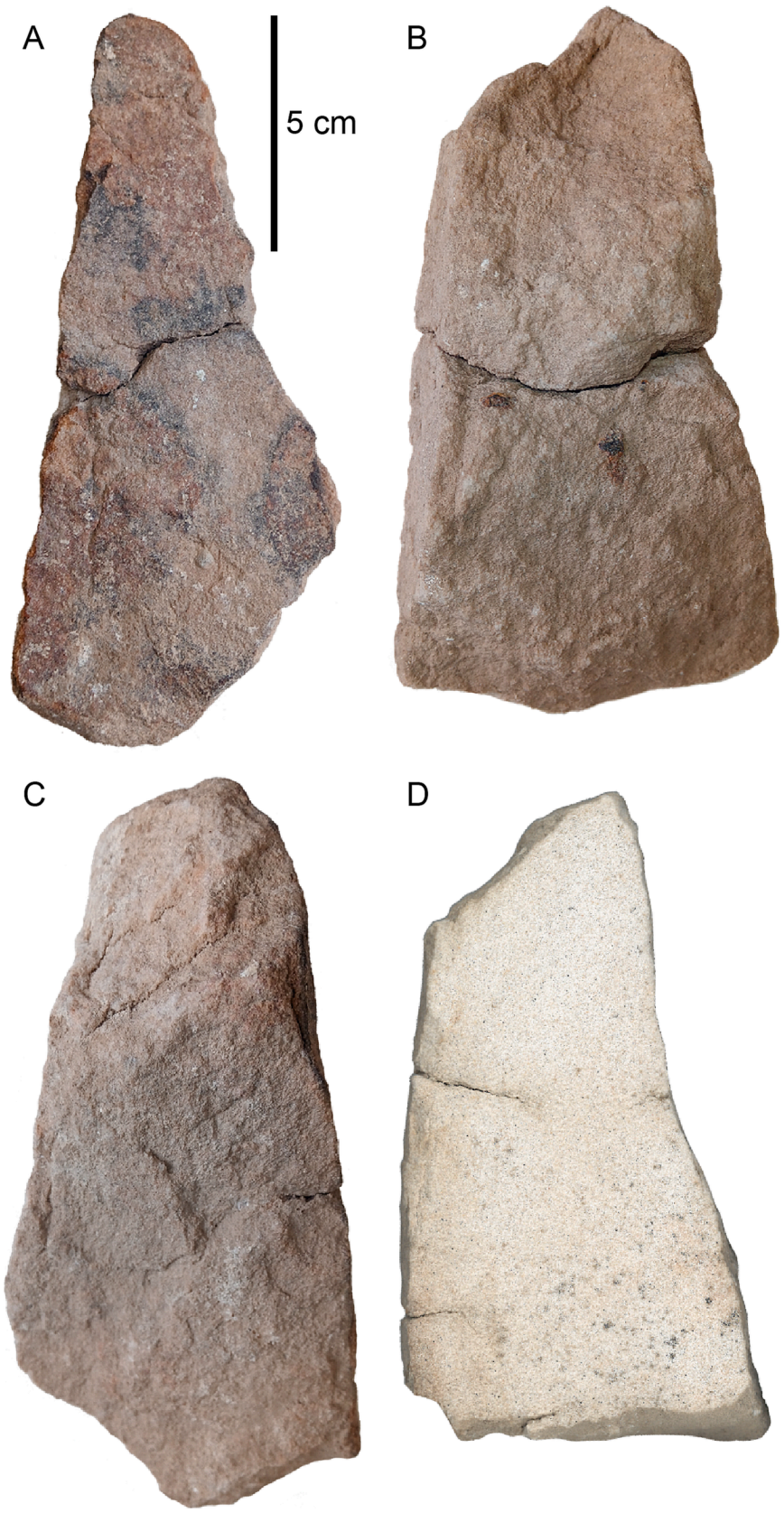

Fig. 3. Photographs of sarsen sample *STH08 C2 (Spit 3) FN549* from trench STH08. A – Ventral view, B – Dorsal view, C – Lateral view, D – View of cut surface across stone's width.

A subset of 54 sarsen fragments was selected for ICP-AES and ICP-MS analysis from the sample population of 1,028 fragments described in Section 3.1.1. Samples were chosen from the assemblages from each of the three excavation trenches (TR44 – 10 samples; TR45 – 12 samples; STH08 – 32 samples) and to encompass the chemical variability revealed by pXRF analysis (see results in Section 4.1).

Samples were processed and analysed by ALS Minerals (Seville, Spain). Each sample was crushed using a hardened steel jaw crusher such that > 70% of the resulting fragments passed through a 2 mm screen size (ALS Geochemistry preparation package CRU-31). The crushed material was then powdered using an agate planetary ball mill such that > 85% passed a 75 μm screen size (ALS Geochemistry package PUL-42).

Major/minor elements were analysed by lithium metaborate fusion digestion and ICP-AES (ALS Geochemistry method ME-ICP06) and are reported in units of wt.% oxide. Trace elements including the Rare Earth Elements (REE) were determined using lithium metaborate fusion digestion and ICP-MS (ALS Geochemistry method ME-MS81). As, Bi, Hg, In, Re, Sb, Se and Te were determined by aqua regia digestion followed by ICP-MS (ALS Geochemistry method ME-MS42). Ag, Cd, Co, Cu, Li, Mo, Ni, Pb, Sc, and Zn were determined by four-acid digestion and ICP-AES (ALS Geochemistry method ME-4ACD81). ICP-MS analyses were conducted using an Elan 9000 instrument, while ICP-AES analyses used a Varian 700 Series instrument. Total C and S were analysed by Leco induction furnace and Leco sulfur analyser (ALS Geochemistry methods C-IR07 and S-IR08 respectively). Loss on Ignition (LOI) was calculated following ignition of sample powders at 1000 °C (ALS Geochemistry method OA-GRA05). During ICP analysis, the Certified Reference Material (CRM) OREAS-121 (https://www.oreas.com/crm/oreas-121/) was analysed eight times, the CRM SY-4 (https://www.nrcan.gc.ca/our-natural-resources/minerals-mining/mining-resources/sy-4-diorite-gneiss/8025) ten times and the CRM GRE-03 (http://www.geostats.com.au/certs/GRE-03.pdf) twelve times.

4. Results of pXRF analyses

In this section, we first present the results of pXRF analyses of the full sample of 1,028 saccharoid sarsen fragments from trenches TR44, TR45 and STH08. To allow comparison, results are considered alongside equivalent pXRF data from the extant sarsen stones at Stonehenge. We then present results from the in-depth investigation of sample *STH08 C2 (Spit 3) FN549*. Data from this block are used to determine the extent of any subsurface weathering of buried sarsen fragments, and to explore whether the presence of a subsoil-weathered patina might affect the whole-rock ICP-AES and ICP-MS data presented in Section 5.

4.1. Geochemistry of sarsen fragments

Illustrative pXRF geochemical data for selected sarsen fragments are shown in Table 1 (full dataset available in **Table S2** in the SOM). The data in Table 1 represent raw count % data and, while internally consistent as a dataset, cannot be directly compared to the whole-rock data presented in Section 5, or be used to quantify the mineralogy of samples. Data for selected elements for all samples are shown graphically in Fig. 4. Also plotted (for comparison) are the pXRF data collected by Nash et al. (2020) at Stonehenge for all 52 extant sarsen uprights and lintels. Data from megaliths were collected using the same device and analytical protocols, and at dates interspersed with the analyses presented here. Methodologically, the two datasets are therefore directly comparable.

Comparison of the pXRF data for sarsen fragments from TR44 and TR45 (Fig. 4) shows that the two datasets are indistinguishable in all elements except Ca, which was below detection limits in all of the fragments from TR44. The analyses of fragments from TR44 and TR45 sit within the geochemical space defined by the more numerous fragments from STH08. The results from STH08 differ from those of TR44 and TR45 in that the sarsen fragments from STH08 contain generally lower counts of Si and higher counts of other detected elements. As all the fragments studied here were prepared and analysed in the same way, this observable chemical difference between the three assemblages is either a product of a more varied sarsen population within the assemblage from STH08, or a difference in soil composition between the three trenches, or a combination of both.

Data for the Stonehenge megaliths collected by Nash et al. (2020) sit apart from, or at the periphery of, the array defined by the sarsen fragments in Fig. 4. In general, the sarsen fragments record higher counts by several orders of magnitude for the major elements associated with clay minerals (i.e. Mn, Fe and Al). The same is true of trace elements that readily adsorb onto clay mineral surfaces (Y and Sr), while other trace elements (Zr, Ti, V and Pb) that are less readily adsorbed onto clay surfaces (Takahashi et al., 1998) show counts more comparable to the non-buried Stonehenge array. This indicates, that even after cleaning, the excavated sarsen fragments from buried contexts retain a veneer of clay minerals on their surface, probably localised within pore spaces, grain boundaries and surface defects of primary mineral grains. This finding alone indicates that the comparison of pXRF data from buried lithic materials with long-exposed stone surfaces is not feasible, at least when using sample preparation methods such as those detailed in Section 3.1.1.

4.2. Geochemistry of test block STH08 C2 (Spit 3) FN549

The results in Section 4.1 show that, where a subsoil-weathered patina is present, pXRF data collected from excavated sarsen fragments cannot be compared directly with equivalent data from exposed dressed stone. Before any determination can be made about the efficacy of ICP-AES and ICP-MS data in characterising the whole-rock geochemistry of excavated sarsen fragments, the penetrative depth and volumetric significance of the patina needs to be understood. If a subsoil-weathered patina penetrates deeply into a sarsen fragment, and is thus volumetrically significant, then it would likely affect the whole-rock ICP-AES and ICP-MS data and mask the original geochemical signature of the buried stone. These factors are investigated using sample *STH08 C2 (Spit 3) FN549*, referred to in this section as the *test block*.

4.2.1. Geochemical differences between the exterior and interior of the test block

Analysis of pXRF data from the test block reveals significant differences between the unweathered interior (UI) and subsoil-weathered patina (WP) of the sarsen (see **Table S3** for full data). Fig. 5 displays a selection of elements, comparing the abundances between the UI and WP. Si is the only major element to occur in higher counts ($\bar{x}_{WP} = 60\%$) in the UI than the WP ($\bar{x}_{WP} = 35\%$), where it does in much more variable counts ($\sigma_{UI} = 1.0$; $\sigma_{WP} = 9.8$). All of the other elements analysed are enriched in the WP relative to the UI. The most notable increase from UI to WP is recorded by Ca, which is below detection limit in all UI analyses, but present in all WP analyses ($\bar{x}_{WP} = 11\%$; $\sigma_{WP} = 3.8$) – this is unsurprising given that the Stonehenge site is underlain by Chalk bedrock and thus calcium up-take in any surfaces in contact with chalk-rich soil must be expected. Fe counts also increase by more than an order of magnitude, from 0.04% ($\sigma = 0.001$) in the UI to 0.45% ($\sigma = 0.2$) in the WP. Elements commonly associated with clay minerals show the greatest count enrichment. For example, Al was not detected in the UI, whereas it was detected in all samples in the WP (1.69%; $\sigma = 0.72$). Trace elements including Sr and Rb increase from below detection limit (Rb) in the UI to 0.0002% in the WP, and from 0.0005% (Sr) in the UI to 0.002% in the WP. Similar large changes are observed in the incompatible trace elements (Th, Y, Nb), while more moderate increases are observed in Zr and Ti. The behaviour of the chalcophile elements is more variable, with Cu and Bi showing higher abundances in the UI, while Ni, Zn and Hg all record higher abundances in the WP. Lastly, the light

Table 1
Representative pXRF data (count %) for selected sarsen fragments from TR44, TR45 and STH08. See Section 2 for sample numbering conventions.

Excavation					Al	+/-	Si	+/-	Ti	+/-	Fe	+/-	Rb	+/-	Sr	+/-	Zr	+/-
SAV08 TR44																		
Context number	**Square**			**Sample**														
005	4			–	1.77	0.08	54.52	0.12	0.101	0.009	0.387	0.004	0.0002	0.0001	0.0009	0.0001	0.0018	0.0001
005	12			–	0.98	0.07	59.75	0.11	0.070	0.008	0.202	0.003	–	–	–	–	0.0054	0.0001
005	13			D	3.76	0.07	61.26	0.10	0.265	0.010	0.313	0.004	–	–	0.0003	0.0001	0.0213	0.0002
005	18			B-3378	4.58	0.08	59.66	0.11	0.155	0.009	2.087	0.010	0.0018	0.0001	0.0017	0.0001	0.0204	0.0002
006	20/1			–	2.36	0.07	57.78	0.11	0.115	0.009	0.464	0.005	–	–	0.0029	0.0001	0.0021	0.0001
006	33/2			–	0.99	0.06	58.84	0.11	0.078	0.008	0.191	0.003	–	–	0.0003	0.0001	0.0040	0.0001
SAV08 TR45																		
Context number	**Square**			**Sample**														
033	61			A	2.01	0.08	53.50	0.13	0.165	0.010	0.252	0.004	–	–	0.0006	0.0001	0.0237	0.0002
038	–			A	4.78	0.10	49.61	0.12	0.159	0.009	0.793	0.006	0.0002	0.0001	0.0008	0.0001	0.0032	0.0001
043	6			C	3.48	0.08	54.39	0.11	0.112	0.008	0.403	0.004	–	–	0.0007	0.0001	0.0026	0.0001
045	5			C	4.17	0.08	56.11	0.11	0.137	0.009	0.697	0.005	–	–	0.0008	0.0001	0.0029	0.0001
045	8			J	4.92	0.08	58.12	0.11	0.142	0.008	0.545	0.005	0.0002	0.0001	0.0008	0.0001	0.0026	0.0001
053	1			B	3.81	0.07	59.04	0.10	0.123	0.008	0.495	0.004	–	–	0.0008	0.0001	0.0028	0.0001
STH08																		
Context number	**Spit**	**Environmental number**	**Find number**	**Sample**														
1	–	–	FN633	A	4.38	0.12	17.52	0.07	0.139	0.011	1.041	0.009	0.0005	0.0001	0.0869	0.0005	0.0074	0.0002
2	1	–	FN198	A	0.65	0.07	45.86	0.11	0.156	0.009	0.134	0.003	–	–	0.0015	0.0001	0.0184	0.0002
2	3	–	FN535	E	2.30	0.08	40.74	0.10	0.537	0.013	0.387	0.004	0.0002	0.0001	0.0016	0.0001	0.0256	0.0002
2	3	–	FN560	A	3.82	0.09	53.07	0.12	0.400	0.012	0.527	0.005	–	–	0.0016	0.0001	0.0605	0.0003
3	1/C	9	FN561	A	2.71	0.08	49.77	0.11	0.082	0.008	0.346	0.004	–	–	0.0005	0.0001	0.0037	0.0001
3	1/G	14	FN648	C	4.27	0.09	21.86	0.07	0.121	0.007	0.843	0.006	0.0005	0.0001	0.0021	0.0001	0.0034	0.0001
3	1/H	22	FN640	A	6.04	0.09	46.96	0.10	0.211	0.009	0.694	0.005	0.0002	0.0001	0.0011	0.0001	0.0108	0.0001
3	2/L	47	FN563	D	2.99	0.07	40.46	0.09	0.109	0.007	0.468	0.004	0.0002	0.0001	0.0016	0.0001	0.0127	0.0001
3	3/N	71	FN491	G	4.43	0.09	44.38	0.10	0.135	0.008	0.633	0.005	0.0002	0.0001	0.0008	0.0001	0.0105	0.0001

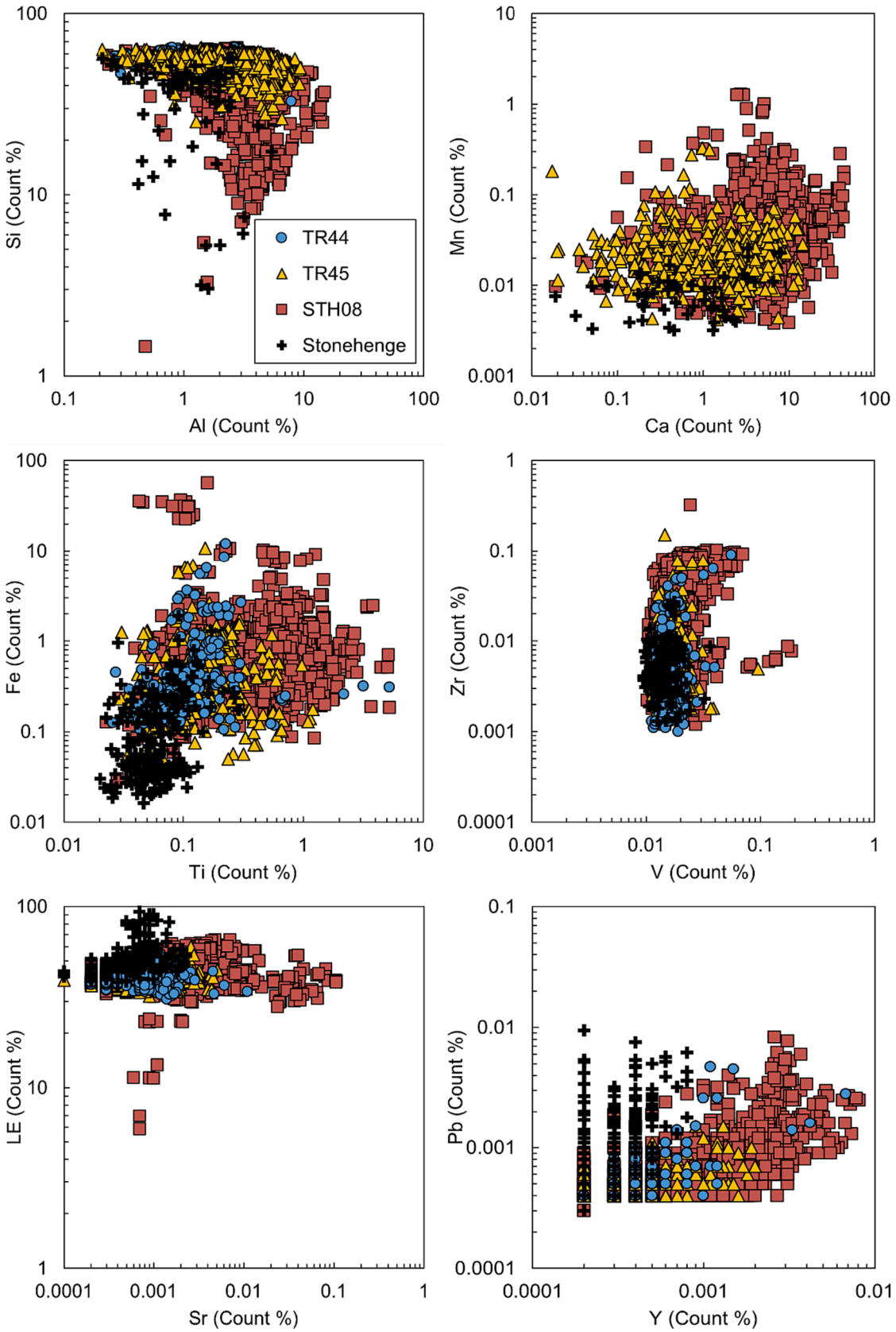

Fig. 4. Bivariate diagrams showing selected elements for sarsen fragments sampled from excavations TR44, TR45 and STH08 at Stonehenge. Ca was below detection limits in all fragments from TR44. Also shown are comparable data for extant sarsen uprights and lintels at Stonehenge (Nash et al., 2020). Units are in raw count %. Analytical error bars are omitted for the sake of clarity. Note that log scales are used in all panels.

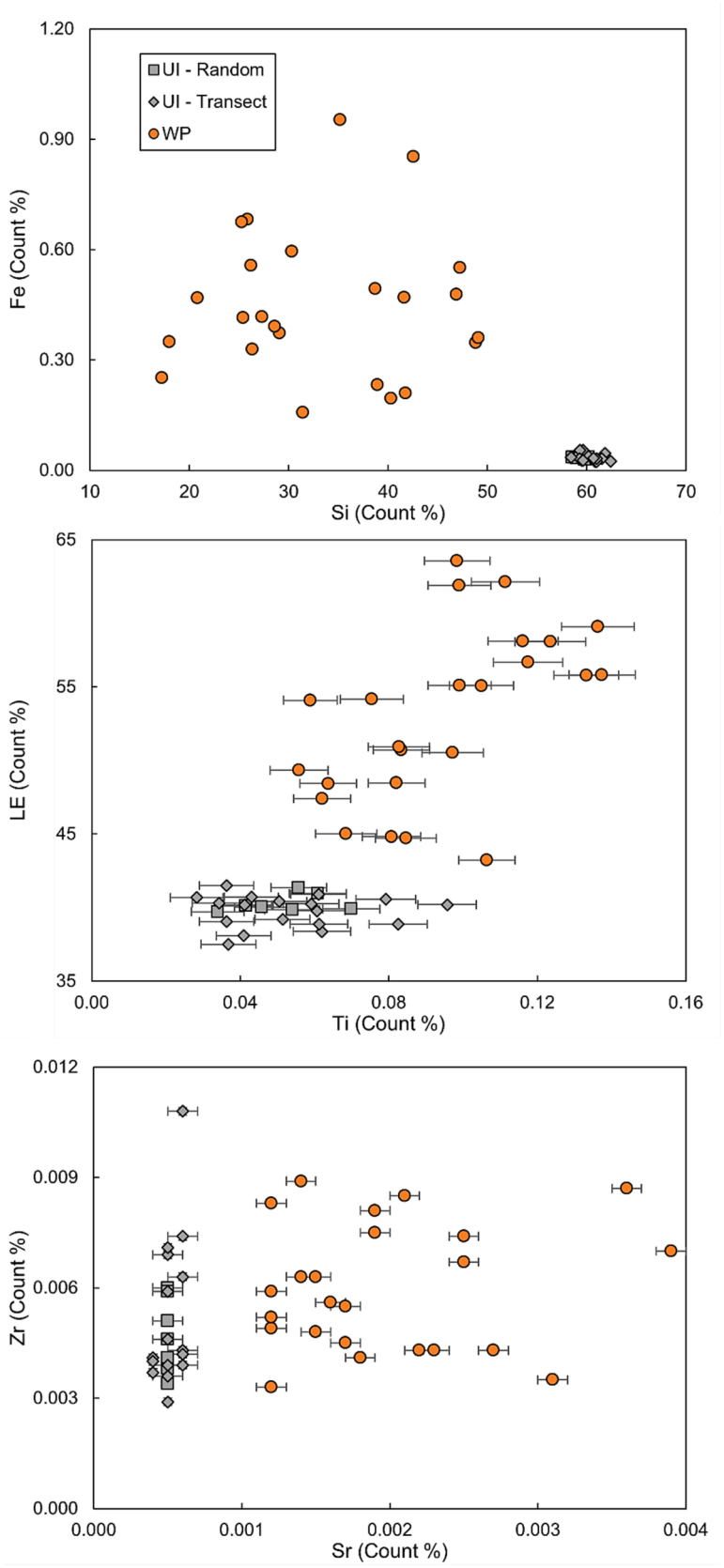

Fig. 5. Bivariate diagram showing geochemical data for the unweathered interior (UI) and subsoil-weathered patina (WP) of sample *STH08 C2 (Spit 3) FN549*. Analysis by pXRF. Error bars are defined by the instrumental accuracy and are recorded automatically during the analysis.

element fraction count (which includes elements with an atomic mass < 11) is always higher and more variable in the WP than the restricted range exhibited by the UI. Element counts between the transect and random analyses (both taken from the UI) are not significantly different.

4.2.2. Modelling the impact of weathered patina thickness upon sample chemistry

The potential effect of variable thicknesses of subsoil-weathered patina on the whole rock geochemistry can be modelled using the average count data for the WP and UI of the test block. This is achieved using a hypothetical sarsen sphere of 30 mm diameter (the smallest analysed in this study; see Section 3.1.1) with an unweathered composition identical to the average UI composition of the test block (Fig. 6**A**). We can replace a variable proportion of the sphere with a weathered patina (identical to the average composition of the WP of the test block). By calculating the volume proportions of the unweathered interior ($V_{UI} = 4/3 \times \pi \times r^3_{UI}$) of the hypothetical sphere to that of its weathered patina ($V_{WP} = [4/3 \times \pi \times r^3_{FRAG}] - V_{UI}$), and multiplying each by their elemental concentration, a hypothetical whole-rock composition can be derived (see Fig. 6**A** for definitions). By adjusting the proportion of UI to WP – in other words, changing the thickness of the patina relative to the unweathered interior – a hypothetical whole-rock composition can be derived and compared to the average composition of the UI of the test block.

The impact of subsoil-weathered patinas of varying thickness on the whole-rock geochemistry is modelled in Fig. 6**B-F**, using Si, Fe, the light element fraction, Sr, Zr and Ti as example elements. What is apparent from this modelling is that the presence of a patina – even a very thin one – can have a comparatively large effect for some elements. Differences between the modelled whole-rock counts of Si, Fe and the light element fraction in the hypothetical sphere and the UI average for the test block are detectable within error limits once the patina reaches ≥ 0.1 mm thickness – i.e., beyond the point where the instrumental error range for the modelled count % for each element (indicated by the y-axis error bars in Fig. 6**B-F**) no longer overlaps with the error range for the same element in the UI of the test block (indicated by the horizontal lines on each plot). For other elements, a much thicker subsoil-weathered patina is needed before the impact on whole-rock counts becomes detectable within error limits. For Sr, the count becomes different from the test block UI average only when the patina reaches ≥ 1.0 mm thickness, whilst for Zr and Ti a ≥ 2 mm thick patina is needed.

The modelling results indicate that geochemical provenancing studies based on major element analyses (e.g. Si and Fe) of small, excavated sarsen fragments are likely to yield spurious outcrop–artefact linkages (if any). This is because the presence of even a minimal subsoil-weathered patina on the surface of a fragment would greatly affect the resulting whole-rock geochemistry. Trace elements (like Sr, Zr and Ti) are less susceptible, but nevertheless require caution in their analysis. Ideally, mechanical sawing or abrasion of excavated fragments would be carried out to remove any patina prior to any geochemical analysis. Alternatively, larger excavated fragments with a volumetrically small patina could be analysed without the need for abrasion, providing – as we do here – the subsequent provenancing study focused solely on trace element geochemistry.

4.2.3. Implications for the use of whole-rock geochemical data

Before we can proceed with the analysis of ICP-AES and ICP-MS data in Section 5, the depth of penetration of the subsoil-weathered patina into the sample sarsen fragments from TR44, TR45 and STH08 needs to be understood. To that end, we re-examine the test block. Visual inspection of the cut surface of the block (Fig. 3**D**, Fig. 7) shows no discolouration that might indicate that a weathering front has penetrated beyond the stone surface. However, it is possible that chemical changes associated with weathering may have advanced ahead of any discolouration front. To test this, pXRF data from the straight-line transect across the cut surface of the block – which started and finished ≥ 1 mm from the block edge – were further inspected.

Geochemical data from the transect are shown in Fig. 7. The analyses from either end of the transect show no appreciable difference in elemental concentrations from any of the analyses taken from the stone interior. Further, none of the analyses along the transect 'trend towards' the weathered patina values with distance from the centre (least likely to be altered) of the block. This finding is important because it demonstrates that the chemical effects associated with patina formation do not extend into the interior of the sarsen to any significant distance. Instead, for the sarsen studied here, the patina is essentially a 2D phenomenon that affects only the outermost surface of the block. For our purposes, we consider the patina to be volumetrically insignificant and unlikely to distort the abundances of trace elements presented in Section 5 and discussed in Section 6.

5. Results of ICP-AES and ICP-MS analyses

Selected whole-rock geochemical data for 30 of the 54 saccharoid sarsen fragments analysed by ICP-AES and ICP-MS are shown in Table 2. Full data are available in **Table S5**, including analyses of certified reference materials.

All of the sarsen fragments are extremely geochemically pure, with SiO_2 > 90 wt. % in all samples ($\bar{x}$ = 98.06 wt. %). In all except four samples (304, 342, 3302 and 3306), Al_2O_3 and Fe_2O_3 occur in abundances < 1 wt. %. These four samples stand out in having significantly more Al, Fe, Mg and K, and less Si (Fig. 8). This difference is most likely due to these samples having a different host mineralogy (pre-silicification) than the other fragments. Differential silicification can be discounted as driving the geochemical difference, because the total Rare Earth Element (REE) abundance of the four samples is not significantly different from the majority, which it would be if silicification was less advanced in these samples.

All 54 sarsen fragments plot as quartz arenites on a SiO_2/Al_2O_3 vs Fe_2O_3/K_2O diagram (Fig. 9), but with samples 304, 342, 3302 and 3306 plotting closer to the sublitharenite boundary. Also shown on Fig. 9 are data for three samples from the interior of Stone 58 at Stonehenge (reported by Nash et al., 2020); these datapoints lie at the approximate median Fe_2O_3/K_2O value of the array of sample fragments from the three excavations, but with higher SiO_2/Al_2O_3 values.

On chondrite-normalised REE diagrams (Fig. 10), the 54 fragments show a uniform enrichment in the lightest REE, with $(La/Sm)_N > 1.90$. The heavy REE element trends are more variable and plot as both positive and negative slopes, with $(Gd/Yb)_N$ ranging between 0.27 and 2.09. The samples show variably negative Eu anomalies, with $(Eu/Eu^*)_N$ in the range 0.22 to 0.96. In comparison to standard crustal end-members, the samples exhibit overall lower REE abundances, likely a dilution effect of silicification. Indeed, some of the samples with the lowest REE concentrations exhibit some 'saw-toothing' in the heavy REE pattern – likely an instrumentation artefact caused by the very low abundances of some elements. Overall, the samples appear to fall into two groups, distinguished on the heavy REE trend: (i) characterised by increasing abundances of the heavy REE with increasing atomic mass, and (ii) by 'flat' heavy REE trends. Also shown in Fig. 10 is the median value for the analyses of Stone 58 at Stonehenge reported by Nash et al. (2020), which is similar to all of the samples in terms of general light REE enrichment, but differs in lacking a significant Eu anomaly. The heavy REE trend of the Stone 58 analysis is relatively flat, most similar to group (ii) above.

When the full trace element geochemistry of the sample fragments is plotted on Upper Continental Crust (UCC)-normalised diagrams (Fig. 11), the compositional variability becomes more apparent. Most of the fragments show significantly negative anomalies in Rb, Sr and Ba, and significantly positive anomalies in Ti, U, Nb, Ta and Zr, as well as positive trends in the least incompatible elements. These fragments are starkly different to any of the sedimentary end-members also presented in Fig. 11, though are generally similar to the analyses from Stone 58 at

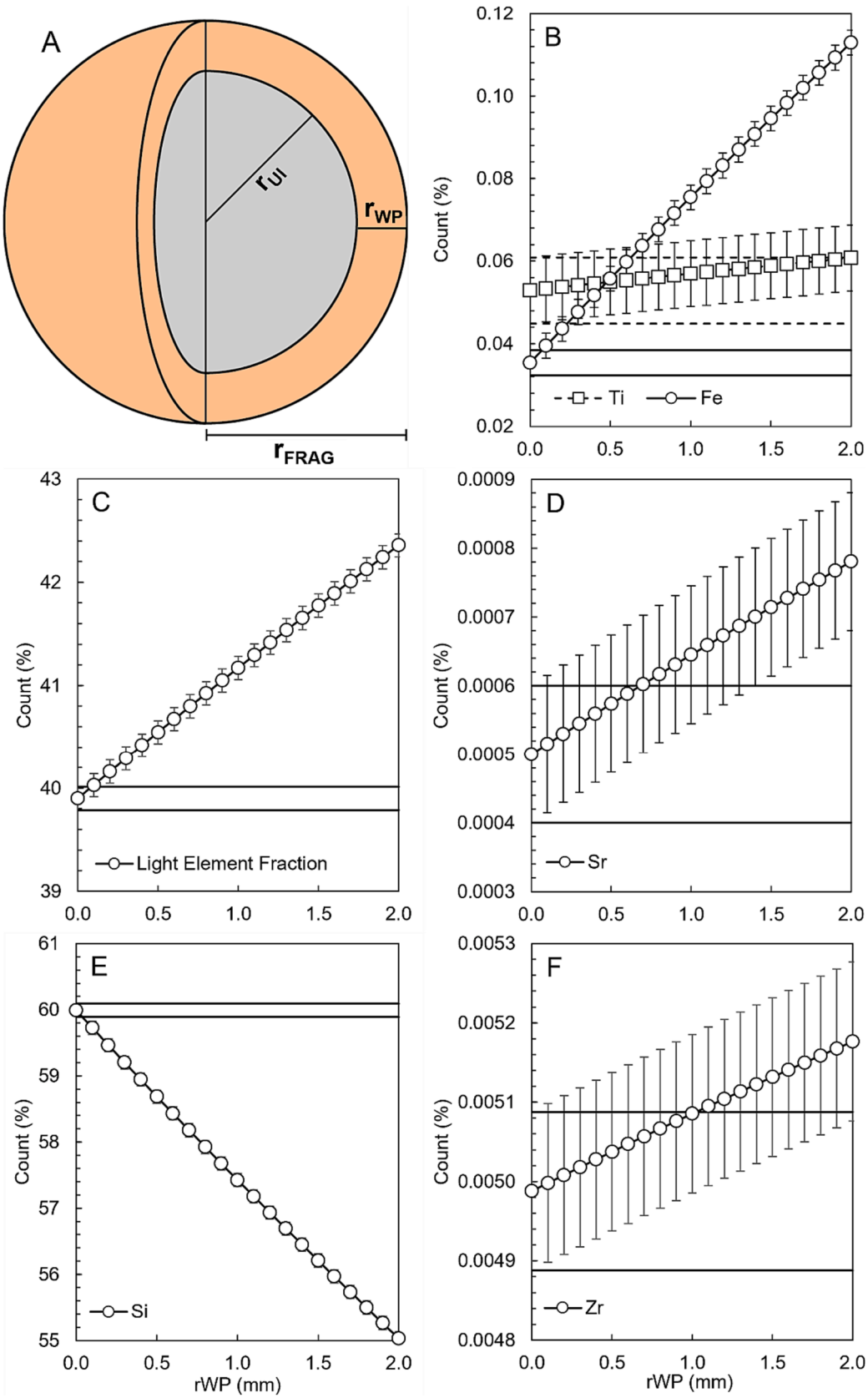

Fig. 6. Visualisation of mathematical model showing (A) how the composition of a hypothetical 30 mm diameter sarsen sphere ($r_{FRAG} = 15$ mm) can be calculated as a product of varying thickness of unweathered interior (r_{UI}) and subsoil-weathered patina (r_{WP}). Panels B-F show the modelled whole rock compositions (count %) for selected elements. Horizontal lines for each element indicate the average composition of the unweathered interior (Fig. 5) plus (upper line) or minus (lower line) instrumental error. Y-axis error bars indicate +/- instrumental error applied to model parameters. Model outputs are available in Table S4 of the SOM.

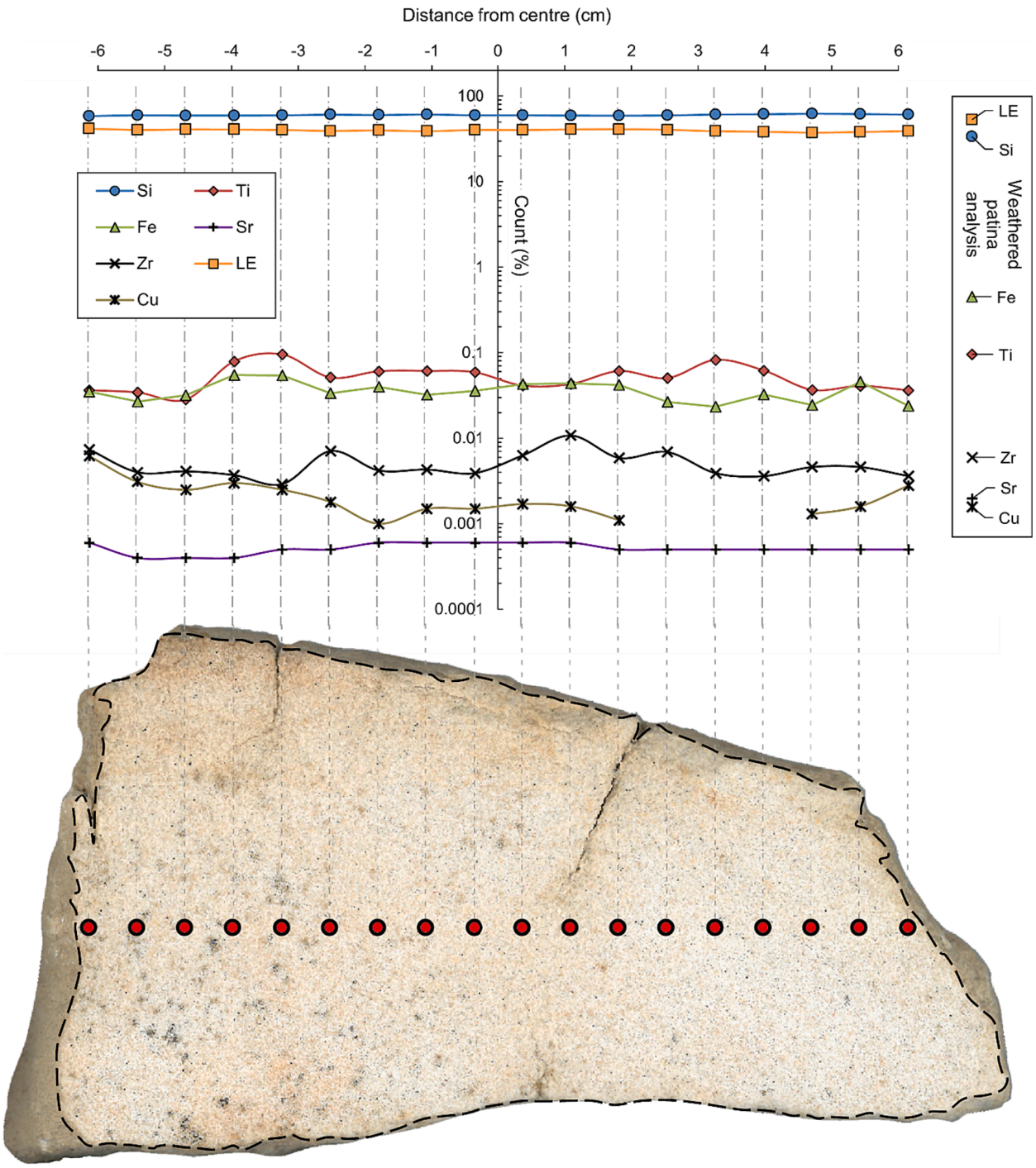

Fig. 7. Variability in geochemical composition (count %) along a transect line across the cut surface of sample *STH08 C2 (Spit 3) FN549* for selected elements. Analyses by pXRF were taken at points shown by circles. Symbols at either side of the plot represent the mean geochemical composition (count %) of the subsoil-weathered patina on the outer surface of the sample. The black dashed line around the sample demarcates the edge of the cut surface from the 3D topography of the block visible in the scanned image.

Stonehenge. Amongst the data is a small set of analyses (304, 342, 3302 and 3306) that are obviously different to the bulk of the other samples. These four analyses – already shown to have a different major element geochemistry to the majority of fragments (Fig. 9) – also lack (i) a strong negative Sr anomaly, (ii) a U anomaly of any kind, (iii) a strong positive Ti anomaly, and (iv) a positive trend in the least incompatible elements, all of which are present in the majority of samples. Instead, this group is most similar to the estimate of Phanerozoic sandstones, having little in common with the analyses of the core from Stone 58.

The differences in trace element chemistry between the different sarsen fragments are most likely driven by differences in the accessory mineral phases within each fragment. The negative anomalies in Rb, Ba and Sr shown by the majority of samples is likely caused by a relative dearth of biotite and feldspars in the sarsen host sediments relative to the UCC. The positive anomaly in Nb and Ti in the majority of the sarsen samples is likely driven by a relative overabundance of rutile, whilst the U and Zr anomalies and positive trends in the heavy REE are likely driven by a relative overabundance of Zr in these fragments. Conversely, the Phanerozoic sand-like signature of the 304–342-3302–3306 group indicates these fragments have a less ‘abnormal’ deportment of the

Table 2
Representative whole-rock ICP-AES and ICP-MS geochemical data for selected sarsen fragments.

Sample	LOI (%)	Major element oxides (wt. %)				Trace elements (ppm)												
		SiO_2	Al_2O_3	Fe_2O_3	TiO_2	Cr	Gd	La	Nb	Rb	Sr	Th	Yb	Zr	U	Nb	Nd	Cu
254	0.41	98.5	0.12	0.13	0.38	20	0.64	1.9	9.4	0.7	4.5	1.40	0.93	291	0.96	9.4	1.3	2
270	0.36	97.4	0.11	0.07	0.02	–	0.23	2.2	0.5	0.9	10.9	0.38	0.09	21	0.28	0.5	1.8	1
288	0.53	98.8	0.15	0.38	0.05	10	0.20	1.3	1.2	0.6	2.4	1.54	0.19	73	0.17	1.2	1.0	5
304	2.31	90.9	1.29	2.41	0.08	40	0.42	3.6	2.7	23.8	16.9	1.02	0.23	132	0.24	2.7	3.0	2
342	2.54	90.6	1.47	3.21	0.11	40	0.71	6.1	2.9	30.6	13.5	2.34	0.42	249	0.47	2.9	5.0	2
401	0.31	98.9	0.08	0.06	0.05	20	0.14	1.2	1.1	0.4	2.5	0.27	0.27	118	0.17	1.1	0.7	–
409	0.39	98.0	0.13	0.40	1.09	50	0.73	2.2	22.8	0.6	15.4	2.29	1.60	501	1.78	22.8	1.9	3
448	0.57	97.7	0.13	0.29	0.77	40	0.63	2.9	16.7	0.5	31.7	1.88	1.61	949	1.80	16.7	1.8	2
1432	0.53	98.4	0.19	0.07	0.06	20	0.44	3.2	1.5	1.2	10.0	0.47	0.24	111	0.19	1.5	3.0	–
1435	0.50	97.8	0.10	0.07	0.87	20	1.02	3.1	19.6	0.4	8.3	1.85	1.42	353	1.17	19.6	2.1	2
1440	0.48	98.6	0.20	0.06	0.05	10	0.31	2.2	1.2	0.9	7.0	0.45	0.17	60	0.12	1.2	2.1	1
1606	0.56	98.0	0.14	0.49	0.37	20	0.55	1.8	8.4	0.5	13.7	1.09	1.01	308	0.81	8.4	1.3	4
1632	0.78	97.0	0.41	0.25	2.85	60	2.59	9.5	67.3	1.3	25.8	6.72	4.22	669	4.82	67.3	6.8	19
1641	0.53	98.7	0.19	0.13	0.79	60	1.15	4.1	15.2	0.6	11.6	2.08	1.78	636	1.54	15.2	3.4	5
1645	0.40	98.7	0.10	0.07	0.56	30	0.56	2.1	11.3	0.6	16.1	1.49	1.21	333	1.11	11.3	1.4	3
1676	0.64	97.3	0.17	0.76	1.51	140	1.69	9.7	32.3	0.7	25.7	3.63	2.70	842	2.61	32.3	6.8	19
1687	0.35	98.5	0.09	0.07	0.48	30	0.33	0.9	10.5	0.3	4.1	1.03	0.99	523	1.04	10.5	0.8	2
1733	0.57	95.9	0.24	0.60	2.20	40	1.66	4.7	51.7	0.8	10.2	4.98	3.75	990	3.64	51.7	3.8	4
3066	0.72	95.6	0.27	0.44	2.01	40	1.97	7.4	45.5	0.7	18.9	4.29	3.20	767	3.01	45.5	6.0	5
3102	0.44	98.5	0.14	0.28	0.86	40	0.57	2.0	16.5	0.6	5.4	1.53	1.10	391	1.31	16.5	1.7	5
3110	0.73	96.4	0.24	0.40	1.90	30	1.49	4.9	40.0	0.8	15.6	3.56	2.54	669	3.02	40.0	3.6	6
3119	0.64	97.0	0.23	0.16	2.13	40	2.11	8.1	46.3	0.8	23.3	4.81	3.45	640	3.22	46.3	6.7	5
3133	0.57	98.6	0.11	0.05	0.09	20	0.19	1.2	2.1	0.6	4.9	0.27	0.37	181	0.32	2.1	0.7	1
3136	0.76	97.4	0.12	0.23	0.08	10	0.19	1.1	1.9	0.7	4.3	0.27	0.25	111	0.26	1.9	0.8	1
3139	0.47	96.5	0.16	0.48	0.88	50	1.00	3.5	16.4	0.6	18.9	2.06	1.69	410	1.55	16.4	2.6	3
3204	0.55	98.7	0.15	0.05	0.05	10	0.34	2.2	1.0	0.9	6.2	0.49	0.14	80	0.20	1.0	1.8	2
3239	0.92	96.0	0.18	0.20	1.48	50	0.83	2.5	27.4	2.1	9.1	2.82	1.68	584	2.02	27.4	2.2	20
3258	0.39	96.4	0.24	0.34	2.25	50	1.64	7.1	44.6	0.9	20.8	4.44	2.94	523	2.81	44.6	5.8	5
3302	1.77	93.9	1.62	2.23	0.16	50	0.57	5.0	4.2	30.4	24.3	1.71	0.43	278	0.58	4.2	4.4	3
3306	1.77	93.1	1.68	2.32	0.17	40	0.41	4.1	4.5	32.2	23.9	1.18	0.38	205	0.48	4.5	3.1	5

accessory mineral phases described above relative to the majority of samples analysed.

6. Discussion

Using complementary methods, the preceding sections have provided a geochemical characterisation of sarsen debitage from TR44, TR45 and STH08 at Stonehenge. pXRF analyses were conducted on 1,028 sarsen fragments (see Section 4). The results indicate considerable overlap in the chemistry of samples, with data for fragments from TR44 and TR45 falling within the geochemical space defined by fragments from STH08. The lack of discrimination between the sarsen fragment samples from the three trenches was attributed to the presence of a subsoil-weathered patina on all fragments, which masks the underlying rock chemistry. In-depth pXRF analyses of the cut surface of a larger sarsen test block from STH08 indicated, however, that this weathered patina is essentially surficial, with no chemical alteration of the rock interior detected. Geochemical modelling work further showed that a patina would need to exceed 1.0 mm thickness before it would have a detectable impact on whole-rock trace element chemistry. With this reassurance, we proceeded with the geochemical characterisation of a subset of 54 sarsen fragments by high-resolution ICP-AES and ICP-MS (Section 5). Analyses of ICP-MS data indicated that compositional groupings may exist within the sarsen debitage, some of which show similarity to Stone 58 at Stonehenge. In this section, we explore the ICP-MS data further to address the two questions raised in Section 1: (i) does the analysed saccharoid sarsen debitage derive from the on-site dressing of Stone 58 (or any of the 49 extant sarsens at Stonehenge with a similar chemical composition to Stone 58); and (ii) what was the original source provenance of the sarsen debitage?

6.1. Does the sarsen debitage derive from the dressing of Stone 58 or a chemically-similar megalith at Stonehenge?

A first step in addressing this question is to determine whether any of the saccharoid sarsen fragments analysed by ICP-MS have the same composition as the majority of extant sarsen megaliths at Stonehenge. To do this, the immobile trace element signature of each of the 54 sarsen fragments analysed here was compared to the equivalent signatures for three samples from the interior of Stone 58 at the monument (see Nash et al., 2021b, for data). The method of comparison, including that used to calculate analytical uncertainty and define $\pm 3\sigma$ error bars, followed that of Nash et al. (2020). As argued in that study, for there to be a permissible match between the immobile trace element signature for a sarsen fragment and that of Stone 58, all 21 Zr-normalised immobile trace element ratios for the fragment and Stone 58 must overlap within the limits of instrumental uncertainty (see Table S6 in SOM for error calculations for current data set).

Using this method, none of the 54 fragments provide a complete match across all 21 trace element ratios with any of the three individual analyses from Stone 58, nor their median or range. Fragment 3258 (excavated from STH08) shows the closest similarity with the median signature for Stone 58, as shown by an overlap for 18 of the 21 trace element ratios (Fig. 12). However, as the Rb/Zr ratio for the fragment is markedly lower compared to the megalith, and the Nb/Zr and Ti/Zr ratios markedly higher, this cannot be considered a permissible match.

The lack of a complete match between any single sarsen fragment and Stone 58 indicates that none of the fragments are debitage from the dressing of Stone 58. By inference, they are also unlikely to be debitage from the other 49 extant sarsens shown by Nash et al. (2020) to be geochemically similar to Stone 58. This suggests that the majority of the extant sarsen megaliths at Stonehenge were dressed at locations other than the excavated areas. An obvious question follows – where are the analysed fragments from? There are five possibilities. First, they could be from another extant megalith. Stones 26 and 160 are potential candidates – shown by Nash et al. (2020) to be chemically different to the other sarsens at the monument and to each other – but without sampling from the interior of these stones, this question remains open. Second, they may be fragments generated during the dressing of one or more of the c.30 sarsen uprights and lintels from Stage 2 of the construction of

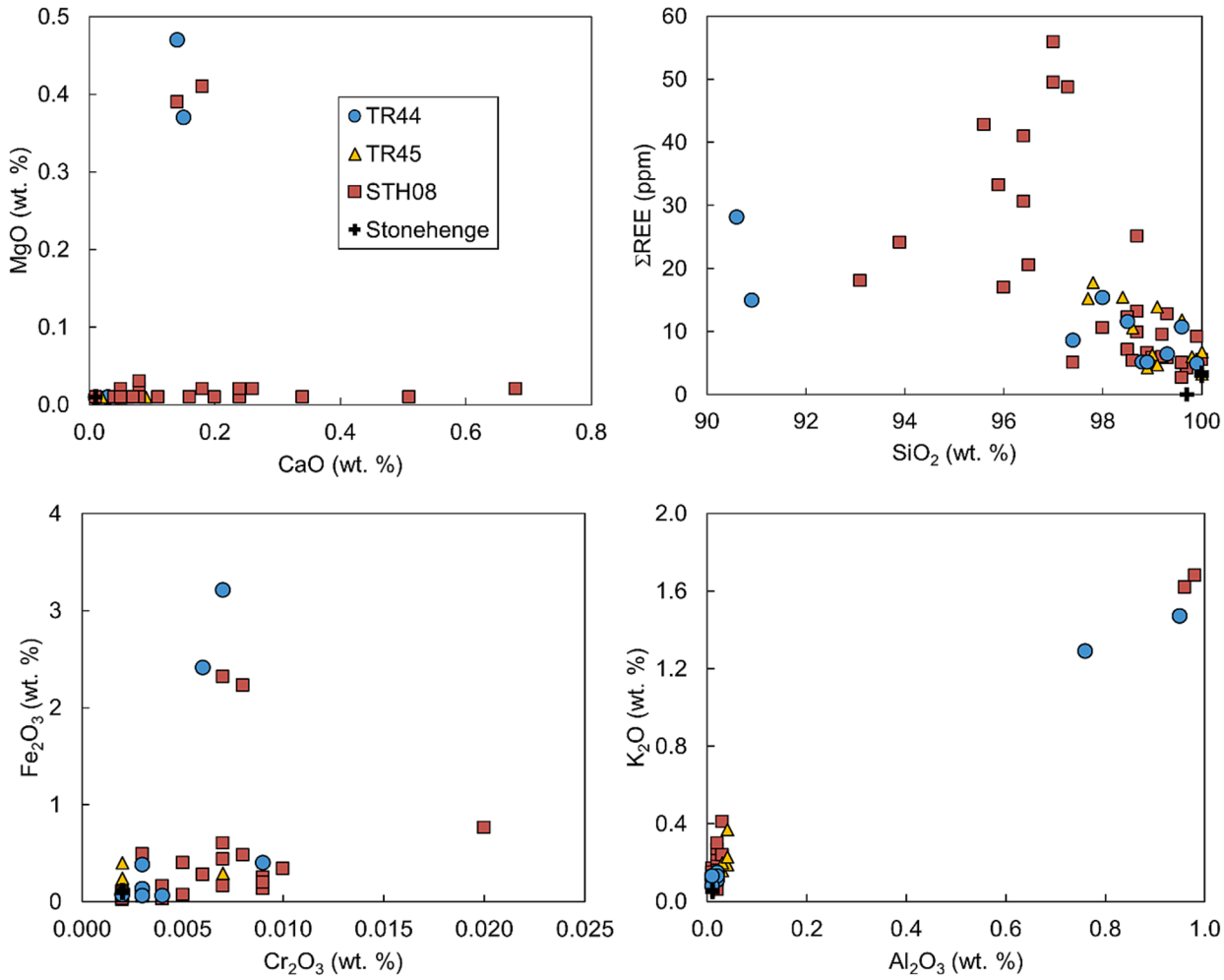

Fig. 8. Bivariate diagrams showing ICP geochemical data for the fragments. Also shown (crosses) are three analyses from the interior of Stone 58 at Stonehenge (data from Nash et al., 2021a).

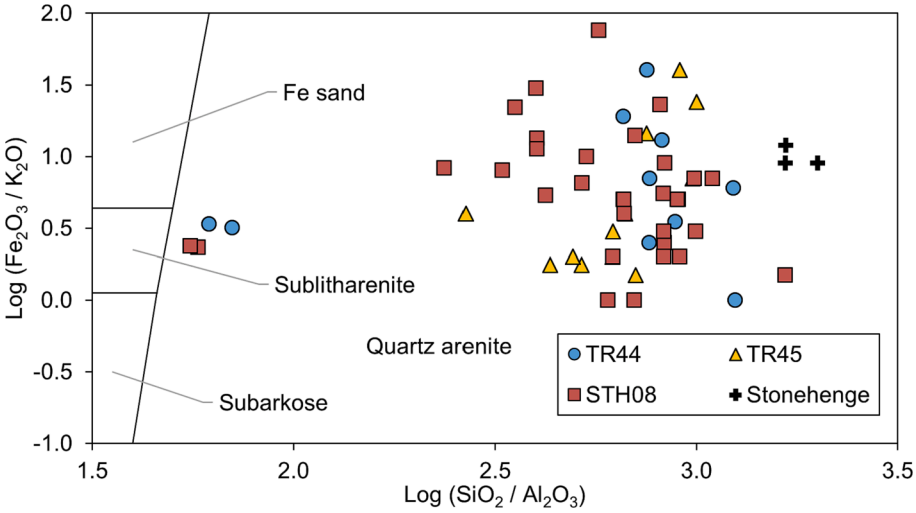

Fig. 9. Log (SiO_2 / Al_2O_3) vs. Log (Fe_2O_3 / K_2O) data for sarsen fragments, differentiated by excavation, alongside equivalent data from the interior of Stone 58 at Stonehenge (Nash et al., 2020). Axes modified after Herron (1988)..

Stonehenge that are no longer present at the monument. Third, some may be debris from broken saccharoid hammerstones. Fourth, some may derive from broken-up sarsen megaliths erected during Stage 1, outside the northeast entrance in Stoneholes B, C and 97 or inside the monument such as in feature WA2321 (Cleal et al., 1995: their Fig. 97) (Fig. 1). Finally, they may represent smaller blocks of saccharoid sarsen brought on-site during the erection of Stonehenge, either as part of the construction process or for some other reason.

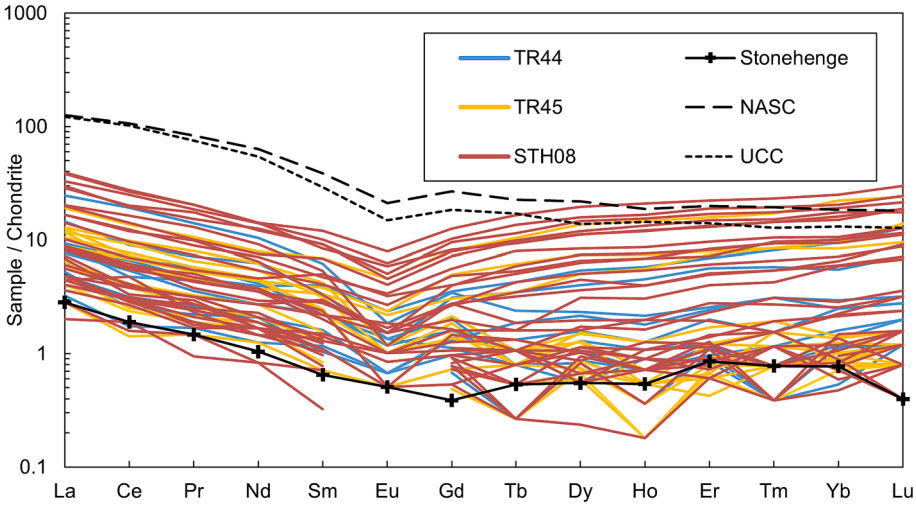

Fig. 10. Chondrite-normalised REE diagram for 54 sarsen fragments, with Upper Continental Crust (UCC; McLennan, 2001), North American Shale Composite (NASC; Gromet et al., 1984) and median data from the interior of Stone 58 at Stonehenge (Nash et al., 2021a) shown for comparison. Normalisation factors from O'Neill (2016).

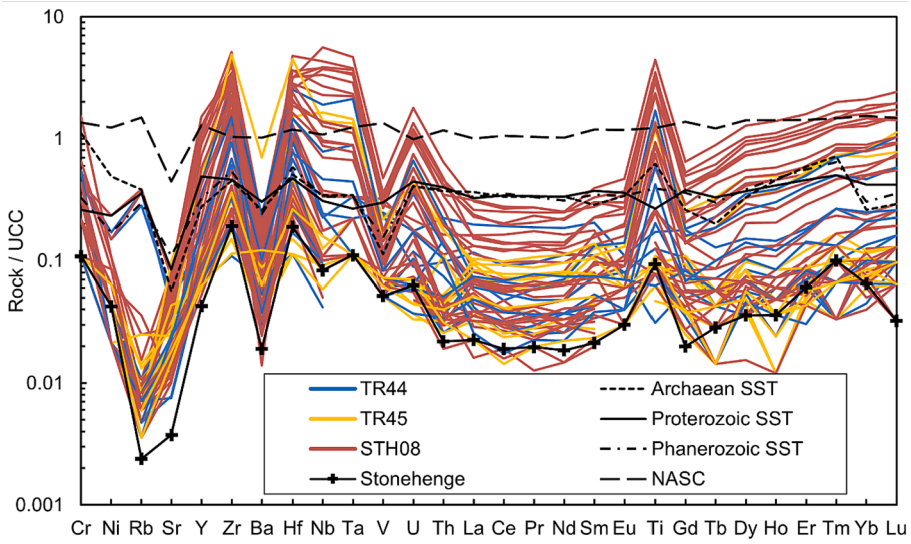

Fig. 11. UCC-normalised trace element diagram for the 54 sarsen samples, with North American Shale Composite (NASC; Gromet et al., 1984), average compositions of Archean, Proterozoic and Phanerozoic sandstones (SST) (Condie, 1993), and median data from the interior of Stone 58 at Stonehenge (Nash et al., 2021a), shown for comparison. Normalising factors from McLennan (2001).

The single sample matching process described above is stringent and does not allow for the very real possibility that compositional variability within a sarsen 'outcrop' may exceed the variation encompassed by the applied analytical uncertainty of a single sample. To address this, the trace element signature of each sample fragment was compared with the other fragments using the method described above. Where two fragments give a permissible match (i.e. 21/21 overlapping trace element ratios), we can argue with confidence that a compositional continuum exists between the two samples (i.e. they are from the same original sarsen block, boulder or outcrop). Where such a continuum is demonstrated, the ranges in trace element ratios of the two samples can be combined and compared to the fragment dataset again. Where any fragments match this extended range, their composition is added to the continuum and the new, expanded continuum is compared again to the dataset. This iterative process, illustrated in Fig. 13, can be repeated until no further matches are achieved.

Using this approach, three continua or 'families' of fragments can be identified (Fig. 14**A**). Together, these families comprise 12 (family ABC1), 8 (D2) and 2 (E) fragments respectively, leaving 32 analyses ungrouped. When the distribution of these families is viewed by excavation (Fig. 14**B**), it is apparent that all three trenches encompass a diverse sarsen assemblage, with each containing fragments from at least two families, but with the majority of fragments ungrouped. Further, fragments from the ABC1 and D2 families are found in all three assemblages, indicating that sarsens of these compositional types were dressed (or used, if the fragments represent pieces moved from where the sarsens were dressed) in all three excavated areas. Following this argument, the excavated area of TR44, interpreted as a dressing floor, may have been used to dress sarsens of varying provenance. It should be noted, however, that the distribution of sarsen debitage in TR44 strongly suggests the dressing of a single monolith in the area of the trench (see Section 2.1). This is to some extent at odds with the presence of sarsen fragments from different 'families'. This may reflect the mixing of sarsen-dressing debris and sarsen hammerstone debris in the excavated area, or perhaps indicates that the debitage in TR44 was partially mixed with material from dressing other sarsens in areas adjacent to the trench.

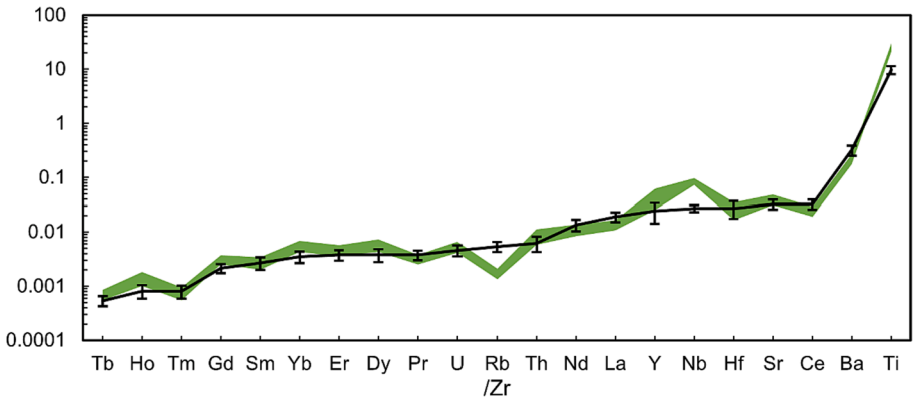

Fig. 12. Zr-normalized immobile trace element ratio data for sarsen fragment 3258 (shaded area) compared to equivalent data from Stone 58 at Stonehenge (solid black line). The upper (lower) boundary for fragment 3258 is defined by the Zr-normalized ratio calculated for each element plus (minus) 3σ of instrumental uncertainty. The solid black line is the median value for each Zr-normalized ratio from three analyses of Stone 58 (Nash et al., 2020). The maximum (minimum) error bars represent plus (minus) 3σ of instrumental uncertainty. Note the overlap between the shaded area and the solid black line for all trace element factors except Rb/Zr, Nb/Zr and Ti/Zr.

Compositional family E is only found in the assemblage from STH08, and may indicate a less-widely used sarsen material.

Just like the comparison of ICP-MS data for individual sarsen fragments, none of the three compositional families overlap entirely with the immobile trace element signature for Stone 58 (Fig. 15). Family ABC1 comes close, overlapping with 20/21 of the trace element ratios. The only difference is for Rb/Zr, which is always higher in the analyses from Stone 58 than in the ABC1 family. This difference cannot be explained by the presence of a subsoil-weathered patina on the ABC1 samples – if anything, any clay fraction present in the patina (within which Rb is compatible) would likely increase the Rb/Zr value for the ABC1 family to above that of the Stonehenge samples, and certainly not lower it. In other words, the difference in Rb/Zr values between the analyses from Stone 58 and the ABC1 family is due to intrinsic differences in the host mineralogy of the sarsens, rather than any surficial effect caused by the subsoil-weathered patina. The lower Rb/Zr values recorded by the ABC1 family are likely driven by lower abundances of minerals such as biotite, chlorite and kaolinite (within which Rb is compatible; e.g. Ewart and Griffin, 1994) in the samples relative to Stone 58. Families D2 and E share only 18 and 12 trace element ratios, respectively, in common with Stone 58, indicating a more distinct mineralogical composition. The lack of overlap between the analyses from Stone 58 and these more compositionally expansive families further strengthens the idea that, although sarsen fragments are well-represented in the three excavated areas, none of the analysed fragments derive from Stone 58 or its chemically equivalent boulders.

6.2. *What was the original source provenance of the sarsen debitage?*

Given the lack of geochemical overlap between Stone 58 (and its chemically equivalent megaliths) and the 54 sarsen fragments analysed, questions regarding the provenance of these fragments arise. To investigate possible sources for the fragments, the 54 individual analyses were compared to the signatures from 20 natural sarsen 'outcrop' areas reported by Nash et al. (2020) (Fig. 16). Using the method described in Section 6.1, it can be shown that three of the fragments from the ABC1 family (334, 1606 and 1645) can be matched to the sarsen outcrop areas at Monkton Down, Totterdown Wood and West Woods, 25–33 km north of Stonehenge on the Marlborough Downs (see Table 3). A further eight fragments from the unassigned group (254, 367, 448, 1641, 1687, 1724, 2761 and 3133) can also be matched to the same three areas. Four fragments match with areas much further from Stonehenge. One fragment from the D2 family (3063) and two ungrouped fragments (3311 and 3314) can be matched with sarsen samples from Hampshire (Bramdean, site 11 on Fig. 16). Ungrouped fragment 1001 overlaps with the composition of sarsens from north of Brighton (at Stoney Wish, site 14). The two fragments that make up the E family match none of the outcrops. From these results, we can infer that sarsen fragments of the ABC1 family were likely brought to Stonehenge from the Marlborough Downs and those of the D2 family from Hampshire.

The presence of sarsen fragments at Stonehenge with a relatively local geochemistry is unsurprising. Nash et al. (2020) showed that sarsen boulders from West Woods were likely used to construct Stonehenge, so it is logical that West Woods, plus Monkton Down and Totterdown Wood (both north of the River Kennet), would be used as sources for other stone. The presence of sarsen fragments with a geochemical signature exotic to the Marlborough Downs is, however, intriguing. Bramdean lies 51 km southeast of Stonehenge, while Stoney Wish is even further to the southeast at 123 km distant. Given the known extent and direction of movement of Quaternary ice sheets, it is impossible that exotic sarsen material was brought to Salisbury Plain from Hampshire and Sussex via glacial transport (e.g. Lee et al., 2011; White et al., 2017; Scourse et al., 2018; Clark et al., 2022). Instead, the only viable explanation is that it was transported there by humans.

The reason why Neolithic people might have brought sarsen to Stonehenge from Hampshire and Sussex is open to speculation. It is possible that the four fragments derive from blocks that were transported and used for purely non-ceremonial purposes (e.g. as a packing stone, or for stone-working alongside hard sarsen hammerstones) – we say blocks (plural) as the fragments do not come from the same compositional family (see Fig. 14). However, this would seem improbable given the ready access to sarsen sources on the Marlborough Downs. Alternatively, it may be that the exotic fragments represent debitage from larger sarsen boulders of ceremonial importance, potentially Stone 26, Stone 160 or a megalith no longer at the monument. The derivation of architectural material from (multiple) exotic sources is already a defining feature of Stonehenge (see Thorpe et al., 1991, and other more recent studies of the Bluestones). This practice could feasibly extend to the sarsen elements of the monument – the derivation of sarsen from multiple sources is already supported by published pXRF data (see discussion in Nash et al., 2020, regarding Stones 26 and 160). Beyond Stonehenge, the use of stone from multiple sources is not uncommon in Neolithic monument building – well-documented examples include Newgrange (e.g. Mitchell, 1992) and several passage graves in the Channel Islands (e.g. Bukach, 2003). Refitting work on the sarsen debitage from STH08 and TR45 would help to establish whether the debitage is from smaller pieces or large blocks. Refitting has identified conjoins in the assemblages recovered from TR44 (see Section 2.1), several of which were characteristic of flakes from dressing a larger boulder. In addition, whole-rock geochemical analysis of Stones 26 and

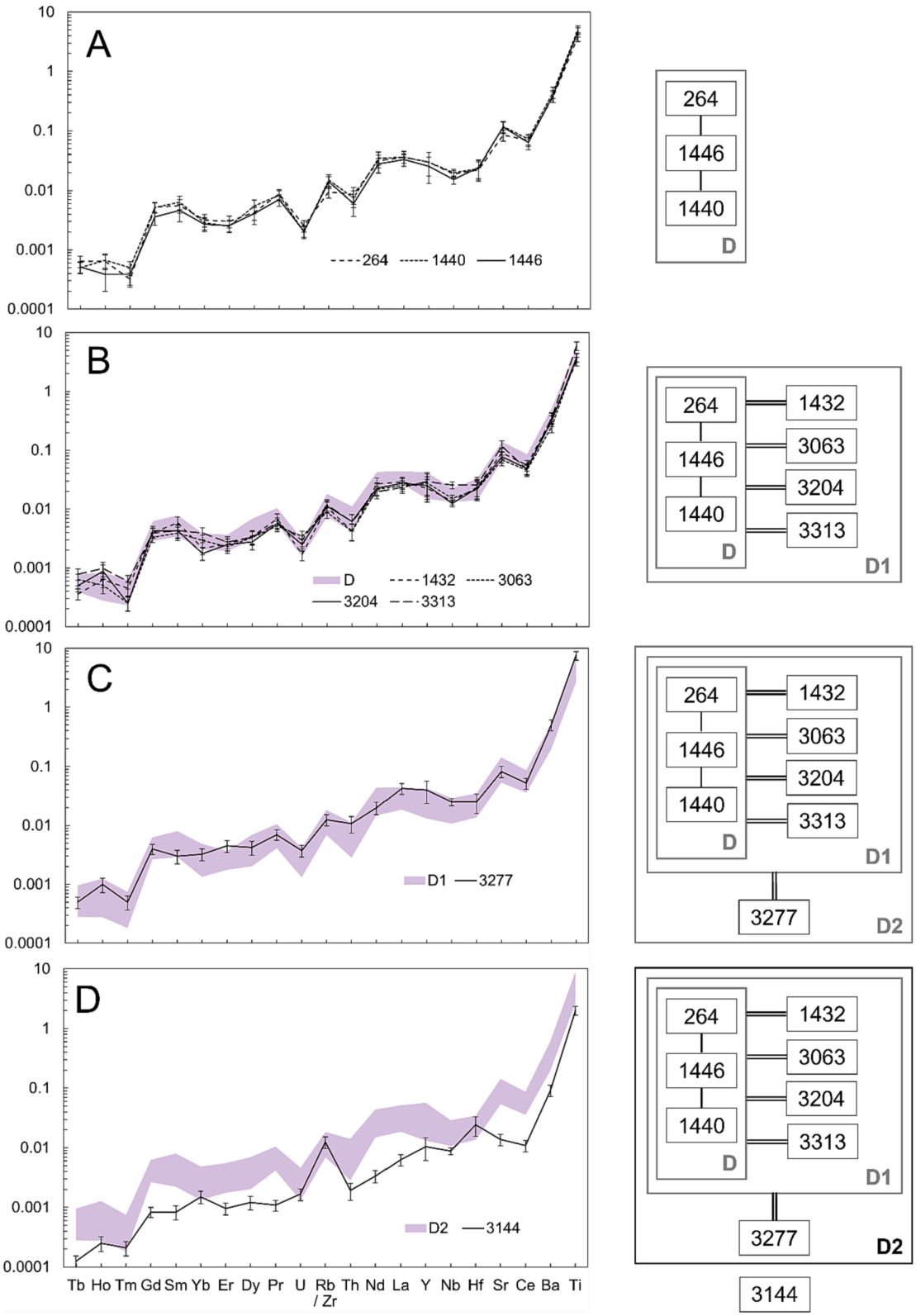

Fig. 13. Diagrammatic representation of the process used to identify a compositional continuum between sarsen fragments, using the D2 family (see text and Fig. 14) as an example. (A) The initial comparison of trace element ratios shows that fragments 264 and 1440 overlap with the composition of fragment 1446, and allows the initial 'D' family to be defined. (B) The extended geochemical range of the D family is compared to the remaining fragments, and provides matches with fragments 1432, 3063, 3204 and 3313, which, when used to extend the geochemical range of the D family, produce the D1 family. (C) D1 is itself compared to the remaining fragments and provides a match with fragment 3277, which, when added to the D1 family, produces D2. (D) D2 is compared to the remaining fragments once more, but yields no further matches (data for fragment 3144 shown as an example).

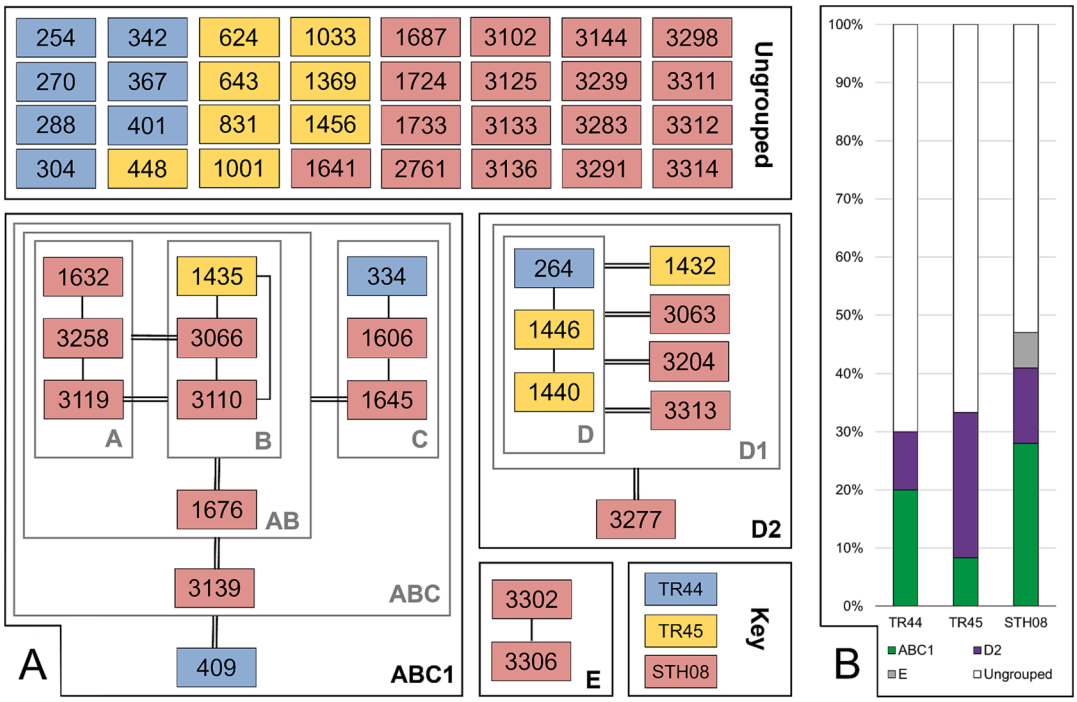

Fig. 14. (**A**) 'Family tree' of Stonehenge fragments showing how the compositional overlap between single samples can be used to define compositional continua (families). Single lines indicate where a geochemical match exits between individual fragments. Double lines indicate where a geochemical match exists between a continuum and a single fragment. Rectangles enclose compositional continua. The iterative processes described in the text yield three compositional continua (families): ABC1, D2 and E. The samples that did not overlap any remain ungrouped. (**B**) Column chart showing the proportion of the three compositional families (and ungrouped fragments) present in the assemblages from the three excavated areas.

160 would be a necessary first step to answer these questions.

The relatively large number of fragments that do not match the chemistry of any of the 20 sarsen outcrop areas sampled by Nash et al. (2020) is understandable. While representing the main areas of sarsen occurrence across southern Britain, sampling was far from exhaustive (especially in the Marlborough Downs area). Further, the compositional range of each sarsen outcrop area was characterised by only three analyses. The implications of this are illustrated by the fact that two fragments from TR44 provide a geochemical match with West Woods, but not with Stone 58 (which itself matches with West Woods). This is a perfectly feasible outcome of our method, and suggests that the West Woods outcrop has a compositional range that extends beyond the three samples used to first characterise it. With an expansion of the sarsen outcrop dataset – a fundamental goal for any future provenancing work on the Stonehenge sarsens – the ungrouped fragments analysed here will likely find a familial 'home'. However, it is important to remember that the distribution of sarsen outcrops in southern Britain has been modified in the recent past. For example, the Kennet Valley and West Woods were centres for sarsen quarrying during the late 19th and early 20th centuries (King, 1968; Whitaker, 2019; 2023), while civic development in Marlborough since 1885 necessitated the removal of sarsen (Pitts, 2022). It is possible that some of the Stonehenge sarsen sources are included in these recent removals and thus might never be identified.

6.3. Archaeological context

The relative and absolute ages of stone-working represented in STH08 and TR44 are currently unconstrained, whereas the sarsen debris from TR45 dates variously to 2310–2220 cal BCE and to before 2580–2280 cal BCE (both at 95% probability; Marshall et al., 2020). It is therefore not certain at what point during the construction of Stonehenge the introduction of much of the sarsen discussed here – either local or exotic – occurred. It is, however, possible to draw some inferences based on the archaeological context of the sampled sarsen fragments.

Table 3 shows the distribution of sarsen fragments that were sourced from specific areas, by excavation, with Fig. 17 plotting the same fragments according to archaeological context. Debitage likely originating from the Marlborough Downs is present in all three trenches. However, sarsen from West Woods occurs only in the assemblage from TR44. As noted in Section 2.1, TR44 is interpreted by Chan et al. (2020) as intersecting a sarsen stone-dressing area. It is therefore possible that a sarsen from West Woods – but not Stone 58 nor its chemically equivalent extant stones – was dressed here, and that the analysed sarsen fragments most likely arrived on site during Stage 2 of monument construction. However, the two fragments from TR44 that can be matched geochemically with the West Woods 'outcrop' are small and technologically undiagnostic. Therefore, as noted above, whether the fragments derive from a megalith or from disintegrated saccharoid hammerstones or from a small sarsen block (such as one of the missing lintels or another small stone brought onsite) is uncertain. In contrast, Fragment 367 in Table 3, which has a match to Monkton Down, is part of the conjoined sarsen flake described in Section 3.1.1 that was likely detached during the dressing of a large sarsen block (see Fig. 2). It therefore seems likely that the sarsen that was being dressed in the area of TR44 was a stone from Monkton Down. No extant megalith at Stonehenge can be matched to the Monkton Down 'outcrop' (Nash et al., 2020), so this absent stone may have been removed or broken up at some time after it was dressed.

The four exotic sarsen fragments shown in Fig. 17 are present in STH08 and TR45. The three fragments that likely originated from Bramdean are from STH08, specifically contexts C2 (the re-excavation of cuttings from Atkinson's 1964 investigations) and C12 (the fill of a Roman pit; see Section 2.2). All three could therefore be residual pieces from prehistoric activity at the site that have become incorporated into later deposits. Possible sources are early stone-breaking, or perhaps fragments of broken hammerstones that became trapped in early surface layers but were later disturbed and reincorporated in later deposits. The

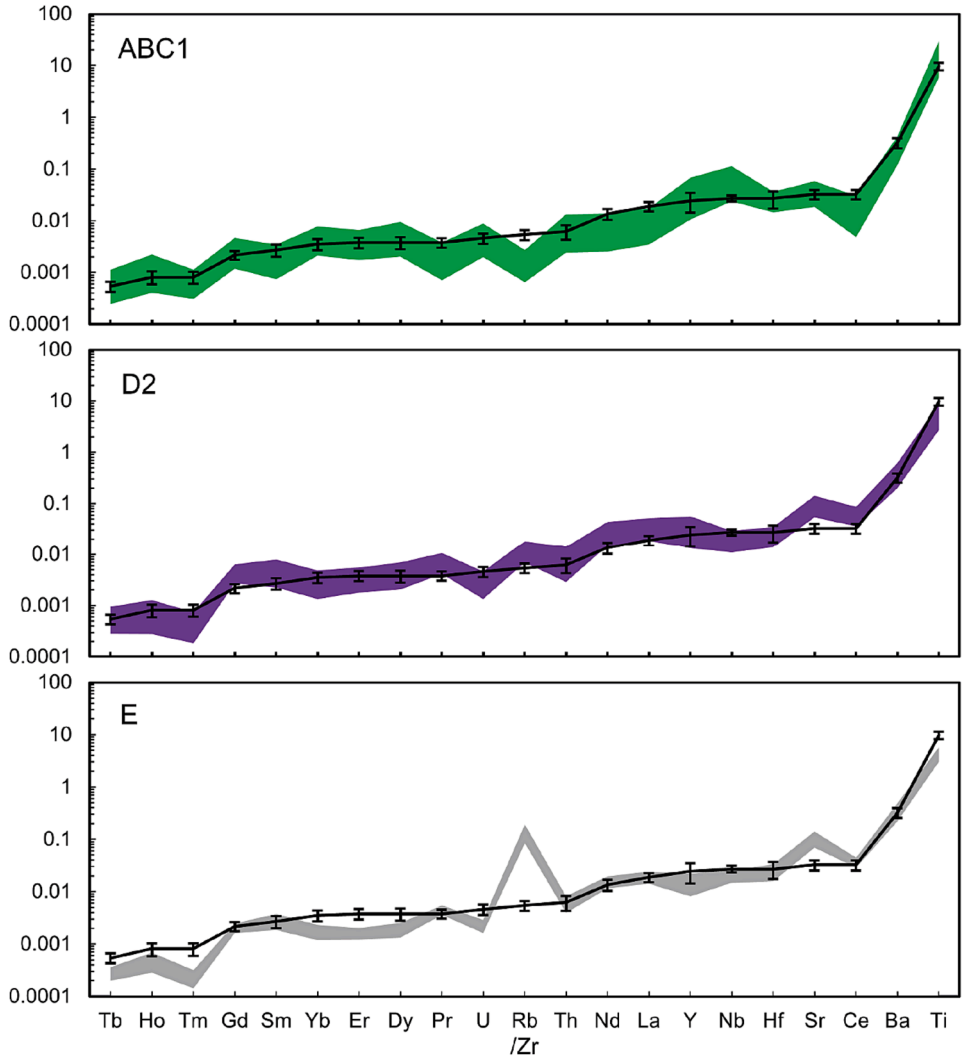

Fig. 15. Zr-normalized immobile trace element ratio data for the three sarsen compositional families identified here (ABC1, D2 and E). Data ranges for the three families are shown by the shaded regions. The upper (lower) boundary for each family is defined by the maximum (minimum) Zr-normalized ratio calculated for each element plus (minus) 3σ of instrumental uncertainty. The solid black line is the median value for each Zr-normalized ratio from the three analyses of Stone 58 (Nash et al., 2020). The maximum (minimum) error bars represent plus (minus) 3σ of instrumental uncertainty.

single fragment from Stoney Wish came from TR45 (within the Avenue bank; see Section 2.1) and thus dates to before 2580–2280 cal BCE (Stage 2/Stage 3 of the development of the monument). Whether it derives from a megalith, from a small block or from a hammerstone is unknown. Its proximity to Stoneholes B, C and 97 raises the possibility that it could derive from a monolith erected early in the construction sequence, placed in any of these holes and dismantled and broken up before Stage 2.

Without knowing the precise time at which sarsen arrived on-site from Hampshire and Sussex, it is only possible to speculate on its role in the development of the monument. Might the exotic sarsen represent an early attempt to employ distant sarsen sources at Stonehenge, similar to the way that the Bluestones were incorporated, only to be abandoned in favour of boulders from the nearby Marlborough Downs? Or could they be the remnants of broken hammerstones brought by the builders of Stonehenge, coming from these distant locations as ready-made tools or as pre-forms? Or could the exotic debitage instead represent the pinnacle of sarsen architecture, where boulders of geographic (and potentially symbolic) significance were brought to the monument and dressed? Alternatively, are the exotic fragments remnants of stones brought from the Bramdean and Stoney Wish areas for either practical or symbolic purpose at different stages of the construction period?

7. Conclusions

This study aimed to use geochemical analysis of sarsen debitage, recovered in 2008 from three excavation trenches at Stonehenge, to expand our understanding of the source provenance of saccharoid sarsen material present at the monument. Using combined pXRF, ICP-AES and ICP-MS analyses, we reach the following conclusions:

a) Through the analysis of 1,028 sarsen fragments by pXRF, we identify that weathering effects, and particularly the development of subsoil-weathered patinas, impact the surface geochemistry of buried sarsen artefacts in such a way that these effects cannot be overcome by simple cleaning. However, such weathering effects are surficial and do not penetrate to any significant depth within the specimens studied here. This is likely due to the particularly inert mineralogy of sarsen. Geochemical modelling indicates that a subsoil-weathered patina would need to exceed 1.0 mm thickness before it would have a detectable effect on whole-rock trace element chemistry. Following cleaning, whole-rock analytical methods such as ICP-AES and ICP-MS will therefore yield geochemical data representative of the primary composition of the material for samples $\geq$ 30 mm diameter.

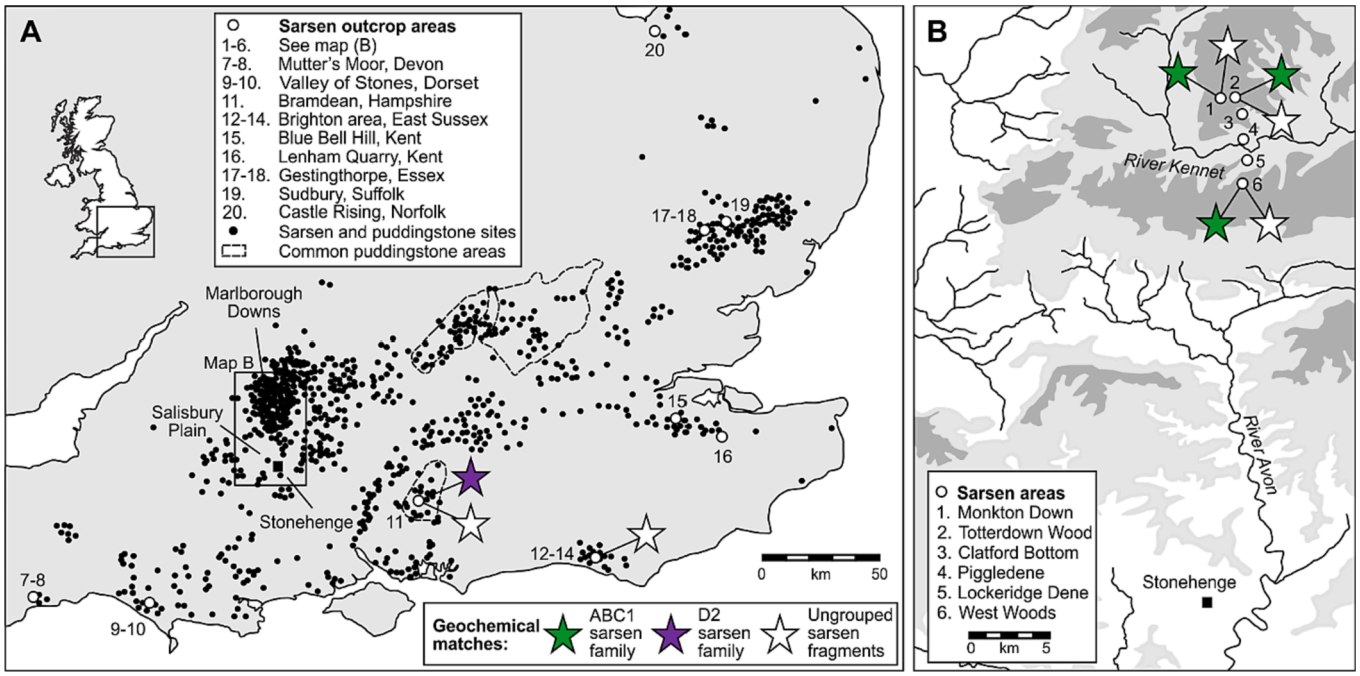

Fig. 16. Geographical distributions of matches between sarsen outcrop areas and geochemically-defined families of sarsen excavated from TR44, TR45 and STH08 at Stonehenge. These distributions are superimposed onto maps of: (A) Distribution of sarsen boulders across southern Britain, including sandy and conglomeratic variants (known as puddingstone); (B) Sampling sites and topography in the Stonehenge-Marlborough Downs area (areas in pale grey at 100 to 175 m above sea level (asl), and those in dark grey at 175 to 270 m asl).

Table 3
Summary of sarsen fragments that provide matches with known areas of sarsen occurrence, organised by excavation. Outcrop numbers follow the site numbering system in Nash et al. (2020) and shown on Fig. 16.

STH08

Fragment	Context number	Spit number	Environmental sample number	Find number	Sub-sample	Sarsen 'outcrop' matches
1606	2	1	–	FN700	C	1. Monkton Down, Wiltshire
1641	2	2	ES3	FN833	D	1. Monkton Down, Wiltshire
1645	2	2	ES3	FN833	E	1. Monkton Down, Wiltshire
1687	2	3	–	FN542	A	2. Totterdown Wood, Wiltshire
1724	2	1	ES2	FN553	B	2. Totterdown Wood, Wiltshire
2761	12	7	–	FN383	A	1. Monkton Down, Wiltshire
3063	12	10	–	FN867	G	11. Bramdean, Hampshire
3133	17	–	ES117	FN800	B	2. Totterdown Wood, Wiltshire
3311	2	3	–	FN549	A	11. Bramdean, Hampshire
3314	2	3	–	FN549	D	11. Bramdean, Hampshire

TR44

Fragment	Context number	Square	Sub-sample	Sarsen 'outcrop' matches
254	005	13	D	6. West Woods, Wiltshire
334	006	43/1	B	6. West Woods, Wiltshire
367	006	74/1	B	1. Monkton Down, Wiltshire

TR45

Fragment	Context number	Square	Sub-sample	Sarsen 'outcrop' matches
448	022	9/1	B	2. Totterdown Wood, Wiltshire
1001	022	25/1	A	14. Stoney Wish, East Sussex

b) Through 54 whole-rock ICP-AES and ICP-MS analyses of representative sarsen fragments, we identify that the immobile trace element signature of none of these fragments overlaps entirely with the equivalent signature for Stone 58 at Stonehenge (data from Nash et al., 2021b). This indicates that the excavated fragments are neither debitage produced during the dressing of this megalith nor, based on arguments put forward in Nash et al. (2020), any of the 49 other chemically similar extant megaliths at the monument.

c) Further inspection of the ICP-MS data reveals that 22 of the 54 sarsen fragments fall into three 'families' (termed ABC1, D2 and E), each with distinct geochemical compositions – the other 32 fragments could not be grouped. None of these families overlap entirely with the immobile trace element signature of Stone 58 and its chemical equivalents at Stonehenge. This implies that sarsen imported from at least a further three locations (in addition to West Woods) is present at Stonehenge. Fragments from the ABC1 and D2 families were found

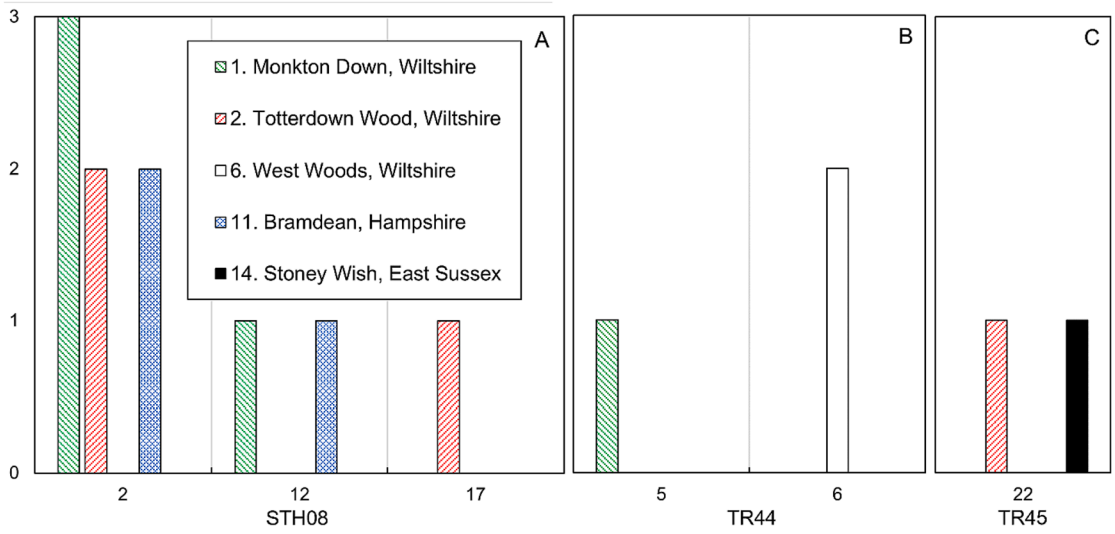

Fig. 17. Delineation of sarsen fragments by archaeological context number for (A) STH08, (B) TR44 and (C) TR45.

in all three trenches, indicating that sarsens of these compositional types were deposited in all three excavated areas, either consecutively or concurrently. Compositional family E is only found in the assemblage from one trench, STH08, within the main Sarsen Circle, and may indicate a less-widely used stone material.

d) Comparison of the immobile trace element signatures for individual sarsen fragments against the equivalent signatures for 20 sarsen outcrop areas across southern Britain (data from Nash et al., 2020), shows that 15 of the 54 fragments can be linked to specific source areas. These include 11 fragments sharing a consistent chemistry with sarsen outcrop areas at Monkton Down, Totterdown Wood and West Woods on the Marlborough Downs. These sites are all relatively local to Stonehenge at 25–33 km north, and – intriguingly – are all situated on the plateau surface of the Marlborough Downs rather than in valley-bottom 'sarsen trains'. Three fragments share a common composition with sarsens at Bramdean (Hampshire), 51 km southeast of Stonehenge, and one with sarsens at Stoney Wish (East Sussex), even further away at 123 km to the southeast. One of the fragments sourced from Monkton Down was part of a large flake likely removed from the outer surface of a sarsen boulder during dressing. This adds a potential second source area for the sarsen megaliths at Stonehenge in addition to West Woods.

At this stage, we can only speculate on the reasons why sarsen stone from such diverse sources is present at Stonehenge. We do not know whether the fragments analysed here represent material removed from (i) the outer surface of Stones 26 or 160 (identified by Nash et al., 2020, as chemically distinct to other sarsens at Stonehenge) or one of the c.30 individual sarsen megaliths erected during Stage 2 of the construction of Stonehenge that are now missing from the monument, or (ii) dismantled and destroyed sarsen megaliths, potentially associated with Stage 1, such as the stones absent from Stoneholes B, C and 97 (outside the northeast entrance) and possible Stonehole WA2321 (in the centre of Stonehenge). With the exception of the fragment from Monkton Down, it is also possible that at least some of the analysed sarsens are instead pieces of (iii) hammerstones or their pre-forms, or (iv) small blocks brought on-site for ceremonial or non-ceremonial purposes.

Such questions can only be answered through further careful refitting of excavated sarsen debitage – but even here, key sarsen fragments will most likely be missing due to the partial excavation of the monument. In the absence of radiocarbon ages for material from TR44 and STH08, we do not know when the sampled sarsen fragments from those trenches were worked on-site. Dating evidence from TR45 suggests that at least some of the sarsen was worked prior to 2580–2280 cal BCE but we do not know whether in Stage 1 or Stage 2 or both. Further lithogeochemical analysis of the 51 uncharacterised sarsen stones at Stonehenge – combined with higher resolution sampling of natural sarsen localities – represents the best way of understanding any further sources for the megaliths. Such efforts should prioritise Stones 26 and 160 at Stonehenge, and sarsen areas within and to the south of the Marlborough Downs.

Whilst focusing exclusively on sarsen from Stonehenge, our results have wider resonance for archaeological provenancing studies. Our key message is that studies attempting to use surficial (pXRF) analysis to provenance any excavated artefact must demonstrate that weathering processes following burial did not significantly alter the primary chemical signature of the material *before* any meaningful provenance interpretations can be made. As our analyses in Section 4 show, even with careful cleaning, the mineralogy of a subsoil-weathered patina effectively masks the composition of the underlying stone. Our pXRF analyses took an estimated 130 h and produced only a small amount of directly useful data – we do not wish other researchers to experience similar levels of disappointment. This message is particularly important for environments where chemical weathering is more intense than in the UK, and for debitage composed of material chemically less resistant than sarsen. The advance of a weathering front into any buried rock fragment depends on intrinsic factors relating to the rock itself (e.g. porosity; permeability; mineralogy), plus environmental factors (e.g. temperature; moisture availability; rainwater, soil and groundwater pH) and the length of time spent in a specific weathering environment. The impacts of lithology and time spent in the weathering environment are especially cogent for Stonehenge where, as noted in Section 1, multiple studies have attempted to source the dolerite Bluestones. Any future attempts to provenance excavated dolerite fragments at the monument (likely derived from the *in situ* dressing of megaliths and/or the removal of flakes in more recent history) must consider differences in the weathering regime experienced by the buried fragments, exposed potential outcrops and standing stones. Due to its mineralogical composition, dolerite is more susceptible to chemical weathering than sarsen. Thus, one should expect differences in weathering to be much more significant between buried dolerite fragments exposed to subsoil weathering, and dolerite outcrops and megaliths exposed to differing intensities and durations of subaerial weathering.

CRediT authorship contribution statement

T. Jake R. Ciborowski: Conceptualization, Data curation, Formal analysis, Investigation, Methodology, Validation, Visualization, Writing

– original draft, Writing – review & editing. **David J. Nash:** Conceptualization, Data curation, Formal analysis, Investigation, Methodology, Validation, Visualization, Writing – original draft, Writing – review & editing. **Timothy Darvill:** Conceptualization, Data curation, Writing – original draft, Writing – review & editing. **Ben Chan:** Data curation, Formal analysis, Validation, Writing – original draft, Writing – review & editing. **Mike Parker Pearson:** Conceptualization, Data curation, Writing – original draft, Writing – review & editing. **Rebecca Pullen:** Data curation, Writing – review & editing. **Colin Richards:** Conceptualization, Data curation, Writing – review & editing. **Hugo Anderson-Whymark:** Data curation, Writing – review & editing.

Declaration of Competing Interest

The authors declare that they have no known competing financial interests or personal relationships that could have appeared to influence the work reported in this paper.

Data availability

All required data is available in the supplementary information attached to the manuscript.

Acknowledgements

General: ALS Minerals (Sevilla, Spain) for ICP-MS and ICP-AES analyses.

Funding

ICP-AES/-MS analyses were supported by British Academy / Leverhulme Trust Small Research Grant SG170610 – 'Geochemical fingerprinting the sarsen stones at Stonehenge'.

Appendix A. Supplementary data

Supplementary data to this article can be found online at https://doi.org/10.1016/j.jasrep.2024.104406.

References

Abbott, M., Anderson-Whymark, H., 2012. Stonehenge Laser Scan: Archaeological Analysis Report. English Heritage Research Report 32–2012, Swindon.

Bevins, R.E., Pearce, N.J.G., Ixer, R.A., 2011. Stonehenge rhyolitic bluestone sources and the application of zircon chemistry as a new tool for provenancing rhyolitic lithics. J. Archaeol. Sci. 38, 605–622.

Bevins, R.E., Ixer, R.A., Webb, P.C., Watson, J.S., 2012. Provenancing the rhyolitic and dacitic components of the Stonehenge landscape bluestone lithology: New petrographical and geochemical evidence. J. Archaeol. Sci. 39, 1005–1019.

Bevins, R.E., Ixer, R.A., Pearce, N.J.G., 2014. Carn Goedog is the likely major source of Stonehenge doleritic bluestones: Evidence based on compatible element geochemistry and Principal Component Analysis. J. Archaeol. Sci. 42, 179–193.

Bevins, R.E., Pirrie, D., Ixer, R.A., O'Brien, H., Parker Pearson, M., Power, M.R., Shail, R. K., 2020. Constraining the provenance of the Stonehenge 'Altar Stone': Evidence from automated mineralogy and U-Pb zircon age dating. J. Archaeol. Sci. 120, 105188 https://doi.org/10.1016/j.jas.2020.105188.

Bevins, R.E., Pearce, N.J.G., Parker Pearson, M., Ixer, R.A., 2022. Identification of the source of dolerites used at the Waun Mawn stone circle in the Mynydd Preseli, west Wales and implications for the proposed link with Stonehenge. J. Archaeol. Sci.-Rep. 45, 103556 https://doi.org/10.1016/j.jasrep.2022.103556.

Bukach, D., 2003. Exploring identity and place: An analysis of the provenance of passage grave stones on Guernsey and Jersey in the Middle Neolithic. Oxf. J. Archaeol. 22, 23–33.

Chan, B., Richards, C., Whitaker, K., Parker Pearson, M., 2020. Sarsens at Stonehenge. In: Parker Pearson, M., Pollard, J., Richards, C., Thomas, J., Tilley, C., Welham, K. (Eds.), Stonehenge for the Ancestors. Part 1: Landscape and Monuments. Sidestone Press, Leiden, pp. 301-357.

Clark, C.D., Ely, J.C., Hindmarsh, R.C.A., Bradley, S., Igneczi, A., Fabel, D., Cofaigh, C.O., Chiverrell, R.C., Scourse, J., Benetti, S., Bradwell, T., Evans, D.J.A., Roberts, D.H., Burke, M., Callard, S.L., Medialdea, A., Saher, M., Small, D., Smedley, R.K., Gasson, E., Gregoire, L., Gandy, N., Hughes, A.L.C., Ballantyne, C., Bateman, M.D., Bigg, G.R., Doole, J., Dove, D., Duller, G.A.T., Jenkins, G.T.H., Livingstone, S.L., McCarron, S., Moreton, S., Pollard, D., Praeg, D., Sejrup, H.P., Van Landeghem, K.J. J., Wilson, P., 2022. Growth and retreat of the last British-Irish Ice Sheet, 31 000 to 15 000 years ago: the BRITICE-CHRONO reconstruction. Boreas. https://doi.org/10.1111/bor.12594.

Cleal, R.M.J., Walker, K.E., Montague, R., 1995. Stonehenge in its Landscape: Twentieth-century excavations. English Heritage, London.

Cochrane, G.W.G., Webb, J.A., Doelman, T., Habgood, P.J., 2017. Elemental differences: Geochemical identification of Aboriginal silcrete sources in the Arcadia Valley, eastern Australia. J. Archaeol. Sci. Rep. 15, 570–577.

Condie, K.C., 1993. Chemical composition and evolution of the upper continental crust: Contrasting results from surface samples and shales. Chem. Geol. 104, 1–37.

Darvill, T., Wainwright, G., 2009. Stonehenge excavations 2008. Antiquaries Journal 89, 1–9.

Darvill, T., Marshall, P., Parker Pearson, M., Wainwright, G., 2012. Stonehenge remodelled. Antiquity 86, 1021–1040.

Darvill, T., Wainwright, G., 2014. Beyond Stonehenge: Carn Menyn quarry and the origin and date of bluestone extraction in the Preseli Hills of south-west Wales. Antiquity 88, 1099–1114.

Ewart, A., Griffin, W.L., 1994. Application of proton-microprobe data to trace-element partitioning in volcanic-rocks. Chem. Geol. 117, 251–284.

Frahm, E., 2013. Validity of "off-the-shelf" handheld portable XRF for sourcing Near Eastern obsidian chip debris. J. Archaeol. Sci. 40, 1080–1092.

Frahm, E., Doonan, R.C.P., 2013. The technological versus methodological revolution of portable XRF in archaeology. J. Archaeol. Sci. 40, 1425–1434.

Frahm, E., Feinberg, J.M., Schmidt-Magee, B.A., Wilkinson, K.N., Gasparyan, B., Yeritsyan, B., Adler, D.S., 2016. Middle Palaeolithic toolstone procurement behaviors at Lusakert Cave 1, Hrazdan valley, Armenia. J. Hum. Evol. 91, 73–92.

Frankel, D., Webb, J.M., 2012. Pottery production and distribution in prehistoric Bronze Age Cyprus. An application of pXRF analysis. J. Archaeol. Sci. 39, 1380–1387.

Gromet, L.P., Haskin, L.A., Korotev, R.L., Dymek, R.F., 1984. The "North American shale composite": Its compilation, major and trace element characteristics. Geochim. Cosmochim. Acta 48, 2469–2482.

Herron, M.M., 1988. Geochemical classification of terrigenous sands and shales from core or log data. J. Sediment. Res. 58, 820–829.

Howard, H., 1982. A petrological study of the rock specimens from excavations at Stonehenge, 1979–1980, in M.W. Pitts, On the road to Stonehenge: Report on the investigations beside the A344 in 1968, 1979 and 1980. Proc. Prehistory Soc. 48, 104–124.

Ixer, R., Bevins, R., 2021. Petrography of sarsen debitage from the Stonehenge Landscape – a broad and perhaps scattered church. Wiltshire Archaeological and Natural History Magazine 114, 18–33.

Jones, T.R., 1887. History of the sarsens. Vegetatio 23, 122–154.

King, N.E., 1968. The Kennet Valley sarsen industry. Wiltshire Archaeological and Natural History Magazine 63, 83–93.

Lee, J.R., Rose, J., Hamblin, R.J., Moorlock, B.S., Riding, J.B., Phillips, E., Barendrecht, R.W., Candy, I., 2011. The glacial history of the British Isles during the Early and Middle Pleistocene: Implications for the long-term development of the British Ice Sheet. In: Ehlers, J., Gibbard, P.L., Hughes, P.D. (Eds.), Quaternary Glaciations – Extent and Chronology, A Closer Look. Elsevier, Amsterdam, pp. 59–74.

Marshall, P., Bronk Ramsey, C., Cook, G., Parker Pearson, M., 2020. Radiocarbon dating of Stonehenge. In: Parker Pearson, M., Pollard, J., Richards, C., Thomas, J., Tilley, C., Welham, K. (Eds.), Stonehenge for the Ancestors. Part 1: Landscape and Monuments. Sidestone Press, Leiden, pp. 527-546.

S.M. McLennan Relationships between the trace element composition of sedimentary rocks and upper continental crust Geochemistry Geophysics Geosystems 2 2001 2000GC000109 10.1029/2000GC000109.

Mitchell, F., 1992. Notes on some non-local cobbles at the entrances to the passage-graves at Newgrange and Knowth, County Meath. J. R. Soc. Antiqu. Irel. 122, 128–145.

Nash, D.J., Coulson, S., Staurset, S., Ullyott, J.S., Babutsi, M., Hopkinson, L., Smith, M.P., 2013. Provenancing of silcrete raw materials indicates long-distance transport to Tsodilo Hills, Botswana, during the Middle Stone Age. J. Hum. Evol. 64, 280–288.

Nash, D.J., Coulson, S., Staurset, S., Ullyott, J.S., Babutsi, M., Smith, M.P., 2016. Going the distance: Mapping mobility in the Kalahari Desert during the Middle Stone Age through multi-site geochemical provenancing of silcrete artefacts. J. Hum. Evol. 96, 113–133.

Nash, D.J., Ciborowski, T.J.R., Ullyott, J.S., Parker Pearson, M., Darvill, T., Greaney, S., Maniatis, G., Whitaker, K.A., 2020. Origins of the sarsen megaliths at Stonehenge. Sci. Adv. 6, eabc0133. https://doi.org/10.1126/sciadv.abc0133.

Nash, D.J., Ciborowski, T.J.R., Darvill, T., Parker Pearson, M., Ullyott, J.S., Damaschke, M., Evans, J.A., Goderis, S., Greaney, S., Huggett, J.M., Ixer, R.A., Pirrie, D., Power, M.R., Salge, T., Wilkinson, N., 2021a. Petrological and geochemical characterisation of the sarsen stones at Stonehenge. PLoS One 16, e0254760.

Nash, D.J., Ciborowski, T.J.R., Salge, T., Damaschke, M., Goderis, S., 2021b. Petrography, geochemistry and mineralogy of the Stonehenge sarsens: Digital data collection [data-set]. Archaeol. Data Service 2022. https://doi.org/10.5284/1084808. Accessed: 7 October.

Nash, D.J., Ciborowski, T.J.R., Coulson, S.D., Staurset, S., Burrough, S.L., Mothualatshipi, S., Thomas, D.S.G., 2022. Mapping Middle Stone Age human mobility in the Makgadikgadi Pans (Botswana) through multi-site geochemical provenancing of silcrete artefacts. Quatern. Sci. Rev. 297, 107811 https://doi.org/10.1016/j.quascirev.2022.107811.

O'Neill, H.S., 2016. The smoothness and shapes of chondrite-normalized Rare Earth Element patterns in basalts. J. Petrol. 57, 1463–1508.

Parker Pearson, M., Bevins, R., Ixer, R., Pollard, J., Richards, C., Welham, K., Chan, B., Edinborough, K., Hamilton, D., Macphail, R., Schlee, D., Schwenninger, J.L., Simmons, E., Smith, M., 2015. Craig Rhos-y-felin: a Welsh bluestone megalith quarry for Stonehenge. Antiquity 89, 1331–1352.

Parker Pearson, M., Pollard, J., Richards, C., Welham, K., 2017. The origins of Stonehenge: On the track of the bluestones. Archaeol. Int. 20, 52–57.

Parker Pearson, M., Pollard, J., Richards, C., Thomas, J., Tilley, C., Welham, K., 2020. Stonehenge for the Ancestors. Part 1: Landscape and Monuments. Sidestone Press, Leiden.

Pearce, N.J.G., Bevins, R.E., Ixer, R.A., 2022. Portable XRF investigation of Stonehenge Stone 62 and potential source dolerite outcrops in the Mynydd Preseli, west Wales. J. Archaeol. Sci.-Rep. 44, 103525 https://doi.org/10.1016/j.jasrep.2022.103525.

Pitts, M.W., 1982. On the road to Stonehenge: Report on the investigations beside the A344 in 1968, 1979 and 1980. Proc. Prehistory Soc. 48, 75–132.

Pitts, M.W., 2022. How to Build Stonehenge. Thames and Hudson, London.

Scourse, J.D., Ward, S.L., Wainwright, A., Bradley, S.L., Uehara, K., 2018. The role of megatides and relative sea level in controlling the deglaciation of the British-Irish and Fennoscandian ice sheets. J. Quat. Sci. 33, 139–149.

Takahashi, Y., Minai, Y., Kimura, T., Tominaga, T., 1998. Adsorption of europium(III) and americium(III) on kaolinite and montmorillonite in the presence of humic acid. J. Radioanal. Nucl. Chem. 234, 277–282.

Thorpe, R.S., Williams-Thorpe, O., Jenkins, D.G., Watson, J.S., 1991. The geological sources and transport of the bluestones of Stonehenge, Wiltshire, UK. Proc. Prehistoric Soc. 57, 103–157.

Tykot, R.H., 2016. Using nondestructive portable X-ray fluorescence spectrometers on stone, ceramics, metals, and other materials in museums: Advantages and limitations. Appl. Spectrosc. 70, 42–56.

Whitaker, K.A., 2019. Sarsen stone quarrying in southern England: An introduction. In: Teather, A., Topping, P., Baczkowski, J. (Eds.), Mining and Quarrying in Neolithic Europe: A Social Perspective. Neolithic Study Group Seminar Papers 16. Oxbow Books, Oxford, pp. 101–113.

Whitaker, K.A., 2023. Sarsen stone quarrying in southern England. Post-Med. Archaeol. 57, 143–176.

White, T.S., Bridgland, D.R., Westaway, R., Straw, A., 2017. Evidence for late Middle Pleistocene glaciation of the British margin of the southern North Sea. J. Quat. Sci. 32, 261–275.